CANMET

Canada Centre for Mineral and Energy Technology

Centre canadien de la technologie des minéraux et de l'énergie

REPORT 79-23

SELECTION OF TERNARY FUSED CHLORIDES FOR THE ELECTROWINNING OF LEAD AND ZINC BASED ON CALCULATED THERMODYNAMIC PROPERTIES

J.M. SKEAFF, C.W. BALE, A.D. PELTON AND W.T. THOMPSON

MINERALS RESEARCH PROGRAM
MINERAL SCIENCES LABORATORIES

Energy, Mines and Resources Canada

Énergie, Mines et Ressources Canada

DECEMBER 1979

Available in Canada through

Authorized Bookstore Agents
and other bookstores

or by mail from

Canadian Government Publishing Centre
Supply and Services Canada
Hull, Quebec, Canada K1A 0S9

CANMET
Energy, Mines and Resources Canada,
555 Booth St.,
Ottawa, Canada K1A 0G1

or through your bookseller

Catalogue No. M38–13/79–23E Canada: $3.25
ISBN 0-660-10667-1 Other countries: $3.90

Price subject to change without notice.

En vente au Canada par l'entremise de nos

agents libraires agréés
et autres librairies

ou par la poste au:

Centre d'édition du gouvernement du Canada
Approvisionnements et Services Canada
Hull, Québec, Canada K1A 0S9

CANMET
Énergie, Mines et Resources Canada,
555, rue Booth
Ottawa, Canada K1A 0G1

ou chez votre libraire.

Nº de catalogue M38–13/79–23E Canada: $3.25
ISBN 0-660-10667-1 Hors Canada: $3.90

Prix sujet à changement sans avis préalable.

FOREWORD

The growing interest in fused salt systems as electrolytes for electrowinning and electrorefining metals as well as for secondary batteries and reaction media has focused attention on the need for thermodynamic data for multi-component systems. At CANMET, fused chloride salt systems are under investigation as possible electrolytes for the electrowinning of molten lead, as well as possible reaction media for the chlorination of sulphide ores.

Because of their generally lower melting temperatures and vapour pressures, multi-component fused salt systems are more suitable as electrolytes and reaction media than are one- or two-component systems. However, obtaining of sufficient experimental data to adequately characterize the thermodynamic properties of multi-component systems may frequently be tedious and time-consuming because of the need to measure a thermodynamic property over wide ranges of compositions and temperatures.

The lack of existing thermodynamic data for ternary and quaternary fused chloride systems of interest at CANMET was recognized in relation to the CANMET Minerals Research Program, Metal Extraction and Refining Project (Project No. 4.3.3.0.04). Recently, however, methods have been developed which enable the calculation of the thermodynamic properties of multi-component systems to be made from a knowledge of the thermodynamic properties of their constituent binary systems. It was to the developers - A.D. Pelton, C.W. Bale and W.T. Thompson of Thermfact Ltd/ Ltée - of one of the more advanced of these methods [The F*A*C*T (Facility for the Analysis of Chemical Thermodynamics) System] that a contract was awarded at the suggestion of P. Pint and J.M. Skeaff of CANMET. The objective of the contract (D.S.S. No. SQ 23440-8-9076) was to calculate the thermodynamic properties of a number of ternary and quaternary fused chloride systems of interest at CANMET as electrolytes and as reaction media. The final report on this contract, entitled "Calculation of liquidus surfaces, vapour pressures and decomposition potentials in certain ternary and quaternary fused salt systems", is the basis of this CANMET Report. Two further CANMET Reports based on the final contract report have as their subject (1) ternary chloride systems for the electrowinning of aluminum and (2) ternary and quaternary chloride systems produced in the chlorination of sulphide ores.

The data contained in this report have been valuable for the CANMET Minerals Research Program. It is furthermore expected that these data will receive wide attention among those in industry, government and universities involved both in fused salt basic research and in the development of processes which employ fused salt media.

Diagrams from the 1964, 1969 and 1975 editions of "Phase Diagrams for Ceramists" are reproduced with the kind permission of the American Ceramic Society, Columbus, Ohio, U.S.A.

W.A. Gow
Chief
Mineral Sciences Laboratories

AVANT-PROPOS

L'intérêt grandissant pour les sels fondus employés comme électrolytes dans les procédés d'électro-extraction et d'électro-affinage ainsi que dans les piles secondaires et milieux de réaction, a créé un besoin de données thermodynamiques sur ce genre de système à plusieurs composants. Pour CANMET les chlorures fondus sont une solution possible pour l'électro-extraction du plomb liquide, ainsi que pour la chloruration de minerais sulfurés.

Parce que leurs températures de fusion et leurs tensions de vapeur sont généralement plus basses, les systèmes de sels fondus à plusieurs composants conviennent mieux comme électrolytes ou milieu de réaction que ceux à un seul ou deux composants. Cependant, il devient très long et ennuyeux d'obtenir les données expérimentales requises pour caractériser adéquatement les propriétés thermodynamiques des systèmes à plusieurs composants, compte tenu de la grande gamme de compositions et températures pour laquelle il faut déterminer une propriété thermodynamique.

Pour leur programme de recherche sur les minéraux et leur projet d'extraction et d'affinage des métaux (No. 4.3.3.1.03), CANMET a dû se pencher sur le problème du manque de données thermodynamiques des systèmes ternaires et quaternaires des chlorures fondus. Récemment, des méthodes ont été mises au point afin de permettre le calcul des propriétés thermodynamiques des systèmes à plusieurs composants en se basant sur les propriétés des systèmes binaires constituants. Les pionniers de ce genre d'investigations qui ont mis au point l'une des méthodes de calcul les plus avancées (A.D. Pelton, C.W. Bale et W.T. Thompson de Thermfact Ltd./Ltée et responsables du système [F*A*I*T (Formulation Analytique Interactive en Thermodynamique)] se sont vus accorder un contrat de CANMET sur la recommandation de P. Pint et J.M. Skeaff. L'objectif de ce contrat était de calculer les propriétés thermodynamiques de plusieurs systèmes ternaires et quaternaires de chlorures fondus. Le rapport final de cette étude portait le titre suivant: "Calculation of liquidus surfaces, vapour pressures and decomposition potentials in certain ternary and quaternary fused salt systems". Il fait l'objet du présent rapport de CANMET. Deux autres rapports de CANMET, basés sur cette même étude, traitaient (1) des systèmes de chlorures ternaires pour l'électro-extraction de l'aluminium et (2) de systèmes de chlorures ternaires et quaternaires produits par la chloruration des minerais sulfurés.

Pour CANMET les données obtenues du rapport final ont été très utiles pour le programme de recherche sur les minéraux. On prévoit de plus que ces données retiendront l'attention des organismes industriels, gouvernementaux et universitaires qui s'intéressent à la recherche sur les sels fondus et au développement des procédés les employant.

Les diagrammes prélevés des éditions 1964, 1969 et 1975 de "Phase Diagrams for Ceramists" ont été reproduits avec la permission de l'American Ceramic Society, Columbus, Ohio, U.S.A.

W.A. Gow
Chef
Laboratoires des sciences minérales

SELECTION OF TERNARY FUSED CHLORIDES FOR THE ELECTROWINNING OF LEAD AND ZINC BASED ON CALCULATED THERMODYNAMIC PROPERTIES

by

J.M. Skeaff*, C.W. Bale**, A.D. Pelton**, and W.T. Thompson***

ABSTRACT

After an extensive literature survey, the available thermodynamic data and phase diagrams of the following binary systems were critically evaluated by a computerized optimization technique: KCl-LiCl, KCl-NaCl, KCl-$PbCl_2$, KCl-$ZnCl_2$, LiCl-$PbCl_2$, LiCl-$ZnCl_2$, NaCl-$PbCl_2$ and NaCl-$ZnCl_2$.

The thermodynamic properties of all known binary phases have been represented by equations, "optimum" binary phase diagrams have been calculated, and error limits have been estimated.

The thermodynamic properties of the following four ternary systems were then estimated from the properties of their binary subsystems by means of interpolation techniques: KCl-LiCl-$PbCl_2$, KCl-LiCl-$ZnCl_2$, KCl-NaCl-$PbCl_2$, KCl-NaCl-$ZnCl_2$.

From these estimated ternary thermodynamic properties, the phase diagrams of the four ternary systems have been calculated. These are presented as polythermal projections of the liquidus surfaces and also as isothermal sections. Comparison to measured ternary diagrams was made in the two cases where reliable data exist. Error estimates are given in all cases.

The estimated ternary thermodynamic properties were also used to generate iso-activity curves for the components $ZnCl_2$ and $PbCl_2$ at several temperatures. From these iso-activity curves, iso-vapour pressure curves and iso-decomposition potentials were calculated from equations given in the text. Tables of standard vapour pressures and standard decomposition potentials have been provided. Error estimates are given in all cases.

Temperatures and compositions of chloride electrolytes suitable for the electrowinning of lead and zinc have been proposed from the isothermal sections of the phase diagrams and from iso-vapour pressure curves.

---

*Research scientist, Process Metallurgy Section, Extractive Metallurgy Laboratory, Mineral Sciences Laboratories, CANMET, Dept. of Energy, Mines and Resources, Ottawa, Canada, K1A OG1; **Départ. de génie métallurgique, Ecole Polytechnique, (Campus de l'Université de Montréal), Montréal, Québec, Canada H3C 3A7; ***Dept. of Mining and Metallurgical Engineering, McGill University, 3480 University St., Montréal, Canada H3A 2A7.

SELECTION DES CHLORURES TERNAIRES FONDUS POUR L'EXTRACTION PAR VOIE ELECTROLYTIQUE DU PLOMB ET DU ZINC EN FONCTION DES PROPRIETES THERMODYNAMIQUES CALCULEES

par

J.M. Skeaff*, C.W. Bale**, A.D. Pelton** et W.T. Thompson***

RESUME

Suite à une étude bibliographique approfondie, les données thermodynamiques et les diagrammes de phase disponibles concernant les systèmes binaires suivants ont été évalués de façon critique par une technique d'optimisation informatisée: KCl-LiCl, KCl-NaCl, KCl-$PbCl_2$, KCl-$ZnCl_2$, LiCl-$PbCl_2$, $LiCl_2$-$ZnCl_2$, NaCl-$PbCl_2$ et NaCl-$ZnCl_2$.

Les propriétés thermodynamiques de toutes les phases binaires connues ont été représentées par des équations, les diagrammes binaires optimum de phases ont été calculés et les limites d'erreur ont été évaluées.

Les propriétés thermodynamiques des quatre systèmes ternaires suivants ont ensuite été évaluées à partir des propriétés de leurs sous-systèmes binaires au moyen de techniques d'interpolation: KCl-LiCl-$PbCl_2$, KCl-LiCl-$ZnCl_2$, KCl-NaCl-$PbCl_2$, KCl-NaCl-$ZnCl_2$.

A partir de ces propriétés thermodynamiques ternaires évaluées, les diagrammes de phases des quatre systèmes ternaires ont été calculés. Ceux-ci sont présentés comme des projections polythermiques des surfaces des liquidus et aussi comme des sections isothermiques. On les a ensuite comparés aux diagrammes ternaires mesurés dans les deux cas pour lesquels des données fiables étaient disponibles. L'évaluation de l'erreur est donnée dans tous les cas.

Les propriétés thermodynamiques ternaires évaluées ont aussi été employées pour engendrer les courbes d'iso-activité pour les composantes $ZnCl_2$ et $PbCl_2$ à plusieurs températures. Les courbes d'iso-tension vapeur et d'iso-potentiel de décomposition peuvent ensuite être calculées à partir des équations données dans le texte. Les tables de tensions de vapeur standards et des potentiels de décomposition ont été fournies. L'erreur est donnée dans tous les cas.

Les températures et les compositions des électrolytes de chlorure convenant à l'extraction par voie électrolytique du plomb et du zinc ont été déterminées à partir des sections isothermiques des schémas de phase et des courbes de pression iso-vapeur.

---

*Chercheur scientifique, section de la métallurgie de procédés, Laboratoire de la métallurgie extractive, Laboratoires des sciences minérales, CANMET, Energie, Mines et Ressources Canada, Ottawa; **Départ. de génie métallurgique, Ecole Polytechnique, (Campus de l'Université de Montréal), Montréal, Qué., Canada H3C 3A7; ***Dept. of Mining and Metallurgical Engineering, McGill University, 3480 University St., Montreal, Canada H3A 2A7.

CONTENTS

TABLES

CONTENTS (cont'd)

FIGURES

CONTENTS (cont'd)

INTRODUCTION

The problems of SO_2 generation and lead emissions associated with conventional lead smelters as well as poor recoveries from certain complex lead-zinc ores have prompted investigation into new processes for lead extraction which would eliminate these difficulties. Areas of investigation which are directed towards the resolution of these problems and which are presently part of continuing research at CANMET are the dry-way chlorination and hydrometallurgical lead processes for the extraction of lead and zinc from complex Zn-Pb-Cu sulphide concentrates by chloride methods. Both of these extraction processes can yield $PbCl_2$ and $ZnCl_2$ which are amenable to fused salt electrolysis for the production of lead and zinc.

Major considerations in the fused salt electrowinning of liquid metals from chloride media are:

1. that the electrolyte be a one-phase liquid;
2. that the electrolyte losses due to volatilization be minimized;
3. that the metal chloride decomposition potential be determined;
4. that the difference in density between the electrolyte and the electrowon liquid metal be sufficient to cause their rapid gravity separation;
5. that the electrolyte have a low viscosity; and
6. that the electrolyte have a high ionic conductivity.

It is thus necessary to have data on phase diagrams, vapour pressures, decomposition potentials, densities, viscosities and electrical conductivities of possible electrolytes in order to determine temperatures and compositions suitable for electrowinning or electrorefining.

In principle, ternary fused salt systems are more suitable as electrolytes than binary systems because in general the former can be expected to exhibit wider regions of complete liquid miscibility, lower melting points and lower vapour pressures of the metal chloride than the latter. However, reliable phase diagram and vapour pressure data for ternary fused chloride systems are frequently lacking because the experimental determination of these quantities is usually tedious and time-consuming due to the need for a large number of measurements. Recently, however, analytical techniques have been developed by three of the authors (C.W.B., A.D.P. and W.T.T.) which enable the calculation of the thermodynamic properties of multi-component systems from the known thermodynamic properties of their constituent binary systems (1).

The objective of the study described in this report was to calculate the phase diagrams, vapour pressures and decomposition potentials in the ternary fused salt systems $LiCl-KCl-PbCl_2$, $NaCl-KCl-PbCl_2$, $LiCl-KCl-ZnCl_2$ and $NaCl-KCl-ZnCl_2$ from the known thermodynamic properties of their constituent binary systems which are listed in Table 1, and based on the results of these calculations, to select electrolyte temperatures and compositions suitable from the viewpoint of:

1. maintaining a one-phase liquid solution for electrowinning of lead and zinc, and
2. maintaining vapour presures of the base metal chlorides low enough to suppress their significant volatilization.

Decomposition potentials give an indication of the minimum applied voltage which will produce lead or zinc metal from the electrolyte. Ternary systems with LiCl and NaCl as the alkali chloride pair were excluded from the study because of the tendency of this combination to hydrolyze which makes them impractical for use as electrolytes.

The first step in the study consists in a computer-assisted critical analysis of the available phase diagrams and thermodynamic data for the binary sub-systems in order to obtain mathematical expressions for the thermodynamic properties of all known phases. At the same time, this critical analysis serves to resolve discrepancies in the literature and to set error limits on all data and calculations. The thermodynamic properties of the ternary systems are estimated from these binary data, and the ternary phase diagrams can then be calculated. The authors have already applied these techniques to calculate the phase diagrams of over 100 ternary chloride (1), fluoride (2), bromide, sulphate, chromate (3), and other fused salt systems. For the eight binary

systems of interest in this study for which measured phase diagrams were available, the calculated and measured diagrams always agreed within or nearly within the reported limits of experimental error.

PURE CHLORIDES

There are five alkali metal or base metal chlorides in the present study. For the phase diagram calculations, their free energies of fusion are required. Values from the literature (4) are listed in Table 2.

BINARY SYSTEMS - GENERAL THEORY

The binary systems which must be analyzed in order to calculate the phase diagrams of all the ternary systems are listed in Table 1.

A thorough literature search of all available phase diagram and thermodynamic data for these systems was performed by Ray MacDonald, Information Officer of CANMET, Energy, Mines and Resources, Canada, using the computerized data bases Chemical Abstracts, Engineering Index, Inspec, SSIE, Conference Papers, CDI and NTIS.

It is necessary to analyze these data in order to obtain mathematical expressions for the thermodynamic properties of all known phases. This involves, firstly, obtaining expressions for the free energies of fusion of all known intermediate compounds in the form:

$$\Delta G^{o}_{fusion} = a + bT + cT^{2} + dT\ln T + eT^{-1} \qquad \text{Eq 1}$$

and then expressing the free energies of formation of these solid intermediate compounds from the pure liquid components as follows:

$$x\ ACl_{(liq)} + (1-x)\ BCl_{(liq)} \rightarrow (ACl)_{x}\ (BCl)_{(1-x)(solid)} \qquad \text{Eq 2}$$

$$\Delta G^{o}_{formation} = a' + b'T + c'T^{2} + d'T\ln T + e'T^{-1} \qquad \text{Eq 3}$$

Table 1 - Systems investigated in the present study

One-component chlorides
LiCl
NaCl
KCl
$PbCl_2$
$ZnCl_2$
Binary systems
KCl-LiCl
KCl-NaCl
KCl-$PbCl_2$
KCl-$ZnCl_2$
LiCl-$PbCl_2$
LiCl-$ZnCl_2$
NaCl-$PbCl_2$
NaCl-$ZnCl_2$
Ternary systems
LiCl-KCl-$PbCl_2$
NaCl-KCl-$PbCl_2$
LiCl-KCl-$ZnCl_2$
NaCl-KCl-$ZnCl_2$

Secondly, expressions must be obtained for the activities of the components as functions of composition and temperature in the liquid phases and in any solid solutions. This is most conveniently accomplished by expressing the molar enthalpy of mixing, ΔH^{mix}, and the excess entropy of mixing S^{E}, as power series in the mole fractions X_A, X_B of the components:

$$\Delta H^{mix} = \sum_{i,j} h_{ij} X_A^i X_B^j \qquad \text{Eq 4}$$

$$S^{E} = \sum_{i,j} s_{ij} X_A^i X_B^j \qquad \text{Eq 5}$$

where h_{ij} and s_{ij} are empirical coefficients found by a least squares curve-fitting procedure. The activities of components A and B are then given by the following expressions (5):

$$\ln a_A = \ln X_A + \frac{1}{RT} \sum_{i,j} (h_{ij} - Ts_{ij})[i + (1-i-j)X_A] X_A^{i-1} X_B^j \quad \text{Eq 6}$$

$$\ln a_B = \ln X_B + \frac{1}{RT} \sum_{i,j} (h_{ij} - Ts_{ij})[j + (1-i-j)X_B] X_A^i X_B^{j-1} \quad \text{Eq 7}$$

For some of the binary systems, ΔH^{mix} has been measured calorimetrically. In other systems, activities in the liquid phases have been measured directly by emf techniques. In each system, measured binary phase diagrams are available. These measured diagrams are of widely varying degrees of accuracy. For some systems, the phase diagrams measured by two or more different authors do not agree with each other. In other systems the measured activities and enthalpies are inconsistent with the measured phase diagram. Hence, a critical analysis must be carried out in which all available data of all kinds (phase diagram, enthalpies, activities, etc.) are considered simultaneously in order to obtain the best optimized set of parameters of Eq 4 and 5 to describe the system. Often, comparisons to other similar systems, the use of structural models, etc. must also be employed in the analysis.

A computer program called *OPTIMISE* has been written to assist in this critical analysis. The different sets of raw data (thermodynamic data, liquidus compositions, etc.) are read directly into the computer interactively along with appropriate weighting factors. The computer program performs a least-squares optimization procedure on all the data. The operator can interact with the program until the thermodynamically most consistent analysis is obtained. This means that in certain cases questionable data may be given a low weighting factor or even rejected.

DETAILS OF ANALYSES OF BINARY SYSTEMS

In this section, the details of the critical analyses are discussed for each binary system. Error limits are given. In Appendix A are found, for each binary system listed alphabetically, the computer-calculated phase diagram and a tabular listing of the coordinates of all calculated phase boundaries on this diagram (the computer-generated diagrams are only given with a resolution of ± 2 mol %, but the tables list the exact compositions). Also given in Appendix A are reproductions of the measured binary phase diagram(s) with references for each system, and in Table A1 a summary of the optimized parameters of Eq 1 to 7 describing the thermodynamic properties of all known phases. Most of the measured diagrams in Appendix A are reproduced from the compilations of "Phase Diagrams for Ceramists" (6), and include the figure numbers of the original text.

KCl-LiCl

ΔH^{mix} was fitted to the accurately measured values of Hersh and Kleppa (7). S^E was determined by fitting the measured phase diagram. Limiting slopes of liquidus curves indicate negli-

Table 2 - Free energies of fusion and melting points of pure chlorides (4)

ΔG°_{fusion} (cal/mol) = a + bT + cT^2 + dTlnT + eT^{-1}

	T_{fusion} (K)	a	b	c x 10^3	d	e x 10^{-5}
KCl	1044	1136.6	51.481	3.0435	- 8.026	0.436
LiCl	883	1056.5	47.16	3.928	- 7.64	
NaCl	1074	1843.6	48.3	2.85	- 7.606	
$PbCl_2$	768	463.5	64.79	4.635	-10.378	
$ZnCl_2$	591	-2263.1	63.469	2.75	- 9.6	

gible solid solubility. The two measured diagrams agree with each other within 5C°. The more recent eutectic temperature of 348°C is more consistent with smooth thermodynamic functions for the liquid phase than is the older value of 354°C.

Probable maximum error of calculated diagram: ± 5C°.

KCl-NaCl

The accurately measured enthalpies of Hersh and Kleppa (7) were used to obtain the expression for ΔH^{mix}_{liquid}. It is assumed that $S^E = 0$ for the liquid. The two most recently measured phase diagrams were then analyzed to give ΔH^{mix}_{solid} with the assumption that $S^E_{solid} = 0$. A simple sub-regular (two-parameter) equation for the enthalpy of mixing of the solid then reproduces, with very good accuracy, the liquidus, solidus, and the solid-solid miscibility gap of the measured diagrams. The measured and calculated liquidus and solidus agree within less than 5C° and less than 10C° respectively. The calculated consolute point agrees with the measured within 10C° in temperature, and in composition within the limits of experimental error. The earlier phase diagram, which agrees with the more recently measured liquidus but not at all with the more recently measured solidus, was ignored because it could not be reproduced with reasonable thermodynamic functions for the solid.

Probable maximum error of calculated diagram: ± 5C° for liquidus
± 10C° for solidus

KCl-$PbCl_2$

ΔH^{mix} has been measured accurately by McCarty and Kleppa (8) up to 50 mol % KCl. These values were extrapolated to pure KCl, and the equation for ΔH^{mix} was obtained by fitting this curve. S^E was then obtained by fitting the diagram of Ugai and Shatillo (6a). This diagram agrees well with the two other reported diagrams. The values of $G^E_{PbCl_2}$ obtained by Hagemark et al (9) by emf measurements at 625°C were also included in the optimized fit. Limiting liquidus slopes indicate negligible solid solubility. Measured and calculated diagrams agree within 5 to 10C°.

Probable maximum error of calculated diagram: ± 5C° to 10C°.

KCl-$ZnCl_2$

S^E for this system was estimated by the equation in Table A1 which passes through a minimum at $X_{ZnCl_2} = 1/3$, as is consistent with the existence of $ZnCl_4^{2-}$ complexes in the melt. ΔH^{mix} was then obtained by an optimization of the measured phase diagrams and the emf data of Robinson and Kucharski (10) who measured $G^E_{ZnCl_2}$ in the liquid. Other published emf data in this system are questionable and were ignored. Although there are positive deviations in $ZnCl_2$-rich solutions, it is unlikely that there is any liquid-liquid immiscibility in this system.

The free energies of fusion of the intermediate compound were obtained by the phase diagram analysis.

Probable maximum error of calculated diagram: ± 5 to 10C° below 450°C
± 20C° above 450°C.

LiCl-$PbCl_2$

ΔH^{mix} for the liquid has been accurately measured by McCarty and Kleppa (8) and their experimental values are well-fitted by the given equation. The measured phase diagram was then used to obtain the expression for S^E. The measured and calculated diagrams agree within 10C°, but in view of the fact that accurate ΔH^{mix} values were used in the calculations, there is reason to believe that the calculated diagram is accurate. Limiting slopes of the liquidus lines indicate that solid solubility is negligible. There have been several electrochemical studies of the liquid phase in which activities of $PbCl_2$ have been measured. These results agree with the present analysis within experimental error limits.

Probable maximum error of calculated diagram: ± 10C°.

LiCl-$ZnCl_2$

The accurately measured calorimetric data of Papatheodorou and Kleppa (11) were fitted to the given equation. For the phase diagram, only the compositions and temperatures of the peritect-

ic and eutectic points are available (12). The equations for S^E and the free energy of fusion of the intermediate compound were then obtained by exactly fitting these two points. The composition of the compound was assumed to be $2LiCl.ZnCl_2$ since the analogue of this compound exists in other alkali chloride-$ZnCl_2$ systems. Solid solubility was assumed negligible as seems reasonable in view of the quite different chemical properties of LiCl and $ZnCl_2$. The calculated $ZnCl_2$-liquidus is probably somewhat too low. There is a good possibility of a liquid-liquid miscibility gap in this system centred on the $ZnCl_2$-liquidus at high $ZnCl_2$ concentrations (say from 2% LiCl to 25% LiCl). If any of the alkali chloride-$ZnCl_2$ systems exhibits such a miscibility gap, the LiCl-$ZnCl_2$ system is the most likely candidate.

Probable maximum error in calculated diagram: ± 25C°.

NaCl-$PbCl_2$

ΔH^{mix} of the liquid has been accurately measured by McCarty and Kleppa (8). The two measured phase diagrams agree with each other within 10C°, but the earlier diagram of Treis (6a) is preferred because it can be represented by simple one-coefficient power series for ΔH^{mix} and S^E, whereas the later diagram cannot. The transformation in $PbCl_2$ at 422°C reported in the later diagram is not given anywhere else in the literature. ΔH^{mix} of McCarty and Kleppa is very well represented by the given one-parameter equation. S^E was then found by fitting the measured diagram of Treis. Limiting slopes of the measured liquidus lines indicate no solid solubility. The thermodynamic properties given by the equations also agree within experimental error limits with the recent emf measurements of Hagemark et al (9) for the liquid at 625°C.

Probable maximum error of calculated diagram: ± 10C°.

NaCl-$ZnCl_2$

S^E for this system was estimated by the equation in Table A1 which passes through a minimum at $X_{ZnCl_2} = 1/3$, as is consistent with the existence of $ZnCl_4^{2-}$ complexes in the melt. ΔH^{mix} and the free energy of fusion of the intermediate compound were then obtained from the measured diagram. There are strong negative deviations from ideality in NaCl-rich solutions and strong positive deviations in $ZnCl_2$-rich solutions. It is possible that a miscibility gap centred on the $ZnCl_2$-liquidus may exist. There are no measured thermodynamic data for this system except for the values of $G^E_{ZnCl_2}$ measured by emf techniques by a number of authors in $ZnCl_2$-rich solutions, but these results are of questionable accuracy.

Probable error of calculated diagram:
± 10C° below 400°C
± 20C° above 400°C.

CALCULATION OF TERNARY SYSTEMS FROM BINARY SYSTEMS

Once all the binary systems have been analyzed, the thermodynamic properties of the ternary systems can be estimated by means of standard interpolation procedures.

The excess Gibbs free energy of a ternary solution can be estimated by either the Kohler equation or the Toop equation:

KOHLER EQUATION:

$$g^E_{(p)} = (1-X_3)^2\, g^E_{(a)} + (1-X_1)^2\, g^E_{(b)} + (1-X_2)^2\, g^E_{(c)} + \Sigma\, \phi_{nmk}\, X_1^n\, X_2^m\, X_3^k \qquad \text{Eq 8}$$

TOOP EQUATION:

$$g^E_{(p)} = \frac{X_1}{X_1 + X_3}\, g^E_{(a')} + \frac{X_3}{X_1 + X_3}\, g^E_{(b')} + (1-X_2)^2\, g^E_{(c')} + \Sigma\, \phi_{nmk}\, X_1^n\, X_2^m\, X_3^k \qquad \text{Eq 9}$$

where, in the 1-2-3 ternary system of Fig. 1, $g^E_{(p)}$ is the integral excess molar free energy at point p in the ternary system, and $g^E_{(a)}$, $g^E_{(a')}$, ... are the excess free energies in the binary systems at the points indicated. X_1, X_2 and X_3 are the mole fractions. The first three terms on the right hand sides of Eq 8 and 9 are "binary terms" and the last terms, $\Sigma\, \phi_{nmk}\, X_1^n\, X_2^m\, X_3^k$ (n,m,k ≠ 0),

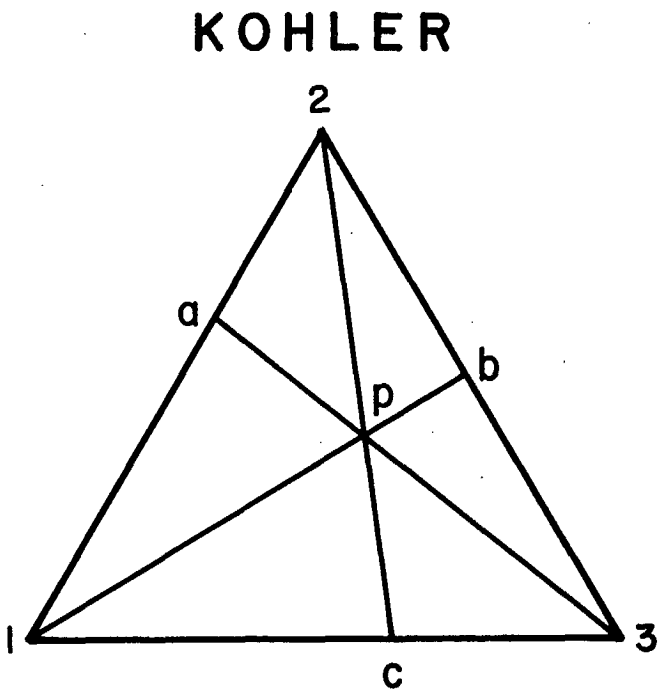

(a)

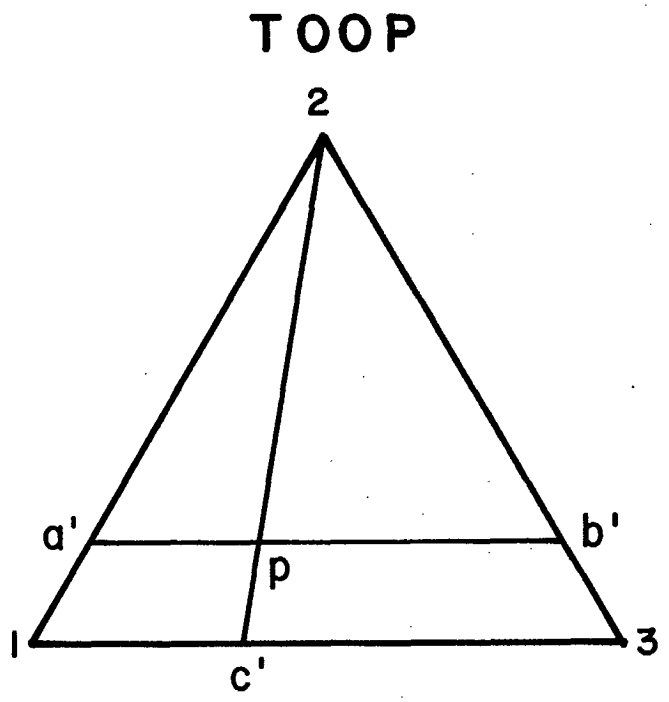

(b)

Fig. 1 - Composition triangle for a ternary system illustrating the geometrical basis of the Kohler and Toop Equations

are "ternary terms" which can be calculated only if data for the ternary system are available. In the present study, the ternary terms are set equal to zero so that Eq 8 and 9 become interpolation formulae for estimating ternary thermodynamic properties from properties of the binary systems.

Both Eq 8 and 9 with ternary terms set equal to zero are exact if the binary and ternary solutions are regular. The equations, with ternary terms set to zero, have been shown by the authors to give a good approximation to the properties of a large number of measured ternary salt systems (1-3).

The Kohler equation has the advantage of being symmetrical with respect to the three components and is thus preferred for charge symmetrical ternary systems such as ACl-BCl-CCl or ACl_2-BCl_2-CCl_2.

For the ternary charge asymmetrical fused salt systems of the type ACl-BCl-MCl_2 under consideration in this study, the Toop equation with ternary terms set equal to zero has been employed. With the asymmetrical component as component 2 in Fig. 1b, the first two terms on the right hand side in Eq 9 represent a linear interpolation between the two asymmetrical binary systems 2-1 and 2-3 at the same mole fraction X_2, while the third term, which is the same as the third term in Eq 8, represents the contribution from the charge-symmetrical 1-3 system.

The use of the Toop equation can also be justified for charge asymmetrical systems on the basis of complex ion models. That is, if it is assumed that the complex anions, MCl_4^{2-}, are formed, Eq 9 with ternary terms neglected can be shown to provide a first approximation for the excess free energy of the ternary solution (1). In this report, only the Toop equation was used, as all the systems are charge asymmetric.

CALCULATION OF TERNARY PHASE DIAGRAMS

Computer-generated polythermal projections of the liquidus surfaces of all calculated ternary phase diagrams are shown in Fig. 2-5. All compositions are given in mole percentages. In Fig. 6 and 7 are shown comparisons between the calculated and measured ternary phase diagram for the systems LiCl-KCl-$PbCl_2$ and NaCl-KCl-$PbCl_2$ which are the only two systems for which reliable measured ternary phase diagrams exist. The agreements between the measured and calculated diagrams are within the limits of experimental error (Note that the calculated diagram for the system LiCl-KCl-$PbCl_2$, Fig. 2 and 6b, is presented with the alkali components as Li_2Cl_2 and K_2Cl_2, in order to facilitate comparison with the measured diagram of Fig. 6a). For the system LiCl-KCl-$PbCl_2$, the two ternary invariant temperatures in the measured diagram are approximately 8C° above those calculated (Fig. 6a and 6b). However, it may be noted that the binary eutectic temperatures reported in the measured diagram are also 6C° above those in the calculated diagram, whereas the calculated diagram agrees with the most recently measured binary diagrams. It should also be noted that the measured phase diagram of the LiCl-KCl-$PbCl_2$ system indicates the existence of a ternary compound. The technique of estimating ternary phase diagrams which is used here cannot, of course, predict the existence of ternary compounds. The compound, however, is weak (the liquidus isotherms are hardly displaced at all when they enter the phase field of the compound). In general it is observed that ternary compounds among chlorides are rare, and where observed they are weak and have little effect on the liquidus surface.

Recently, Shanks et al (13) have measured phase diagrams for the $ZnCl_2$-LiCl-KCl and $ZnCl_2$-NaCl-KCl systems. The measurement technique consisted in the visual observation of the formation of the first crystals in solutions cooled in air in a Pyrex container. The reported binary eutectic and peritectic temperatures differ by about 20C° from those reported by other authors, and the authors themselves (13) give their precision as only ± 17C°, stating that they prefer the binary phase diagrams reported elsewhere. Hence, it is considered that the calculated ternary diagrams reported here for these two systems are probably more accurate than the measured diagrams reported in (13).

As a general rule, to obtain the probable maximum error of a calculated phase diagram

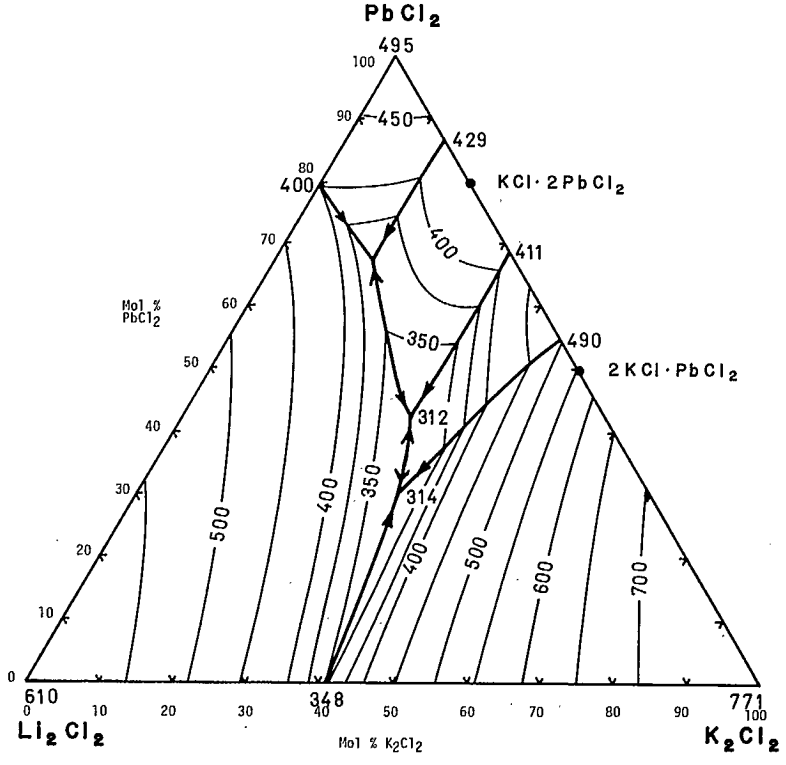

Fig. 2 - Calculated ternary phase diagram of LiCl-KCl-$PbCl_2$

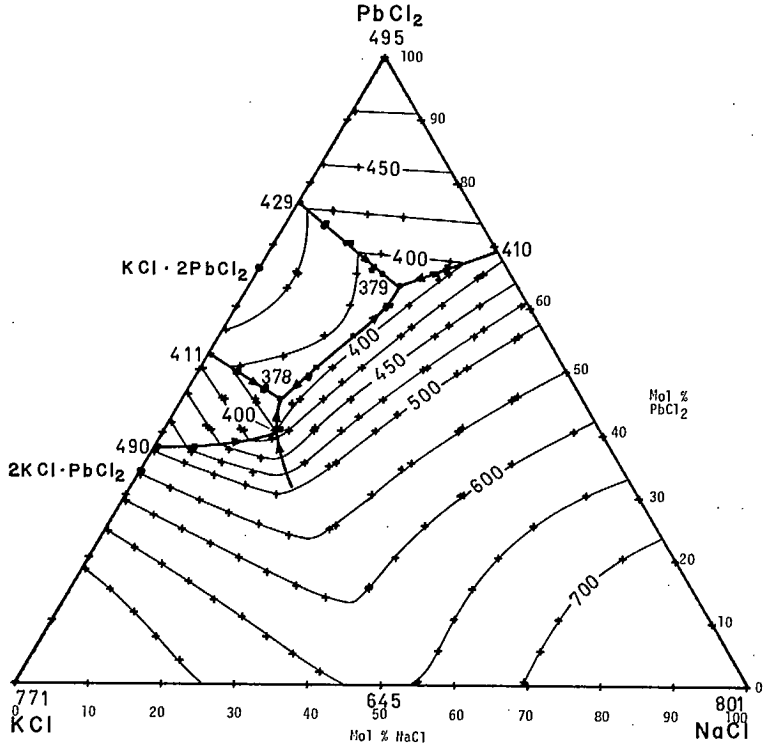

Fig. 3 - Calculated ternary phase diagram of NaCl-KCl-$PbCl_2$

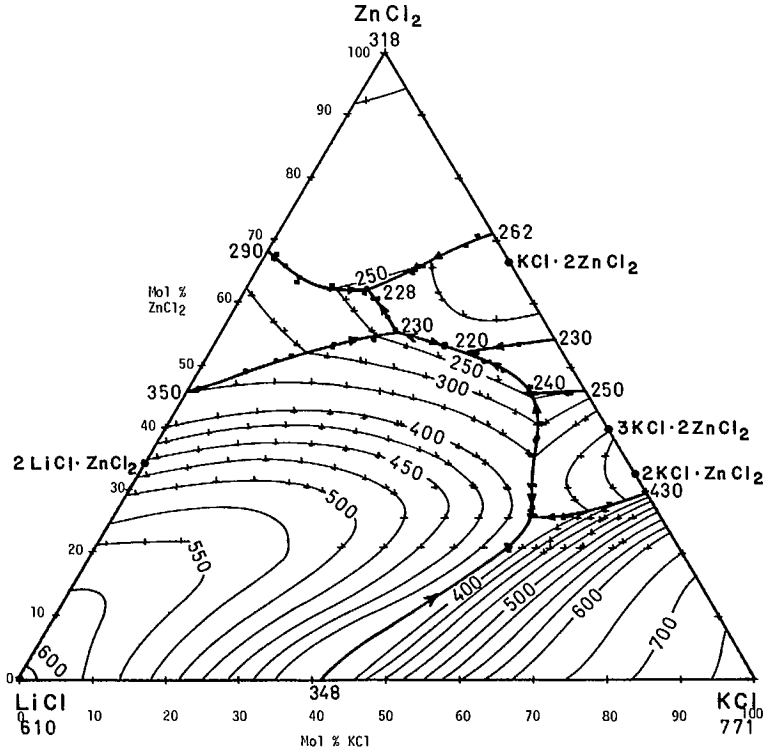

Fig. 4 - Calculated ternary phase diagram of LiCl-KCl-$ZnCl_2$

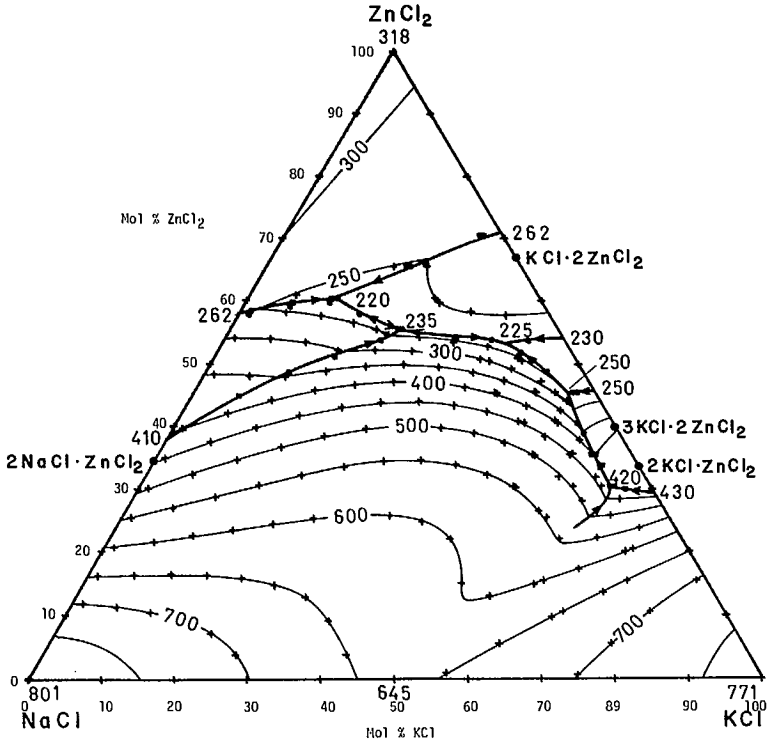

Fig. 5 - Calculated ternary phase diagram of NaCl-KCl-$ZnCl_2$

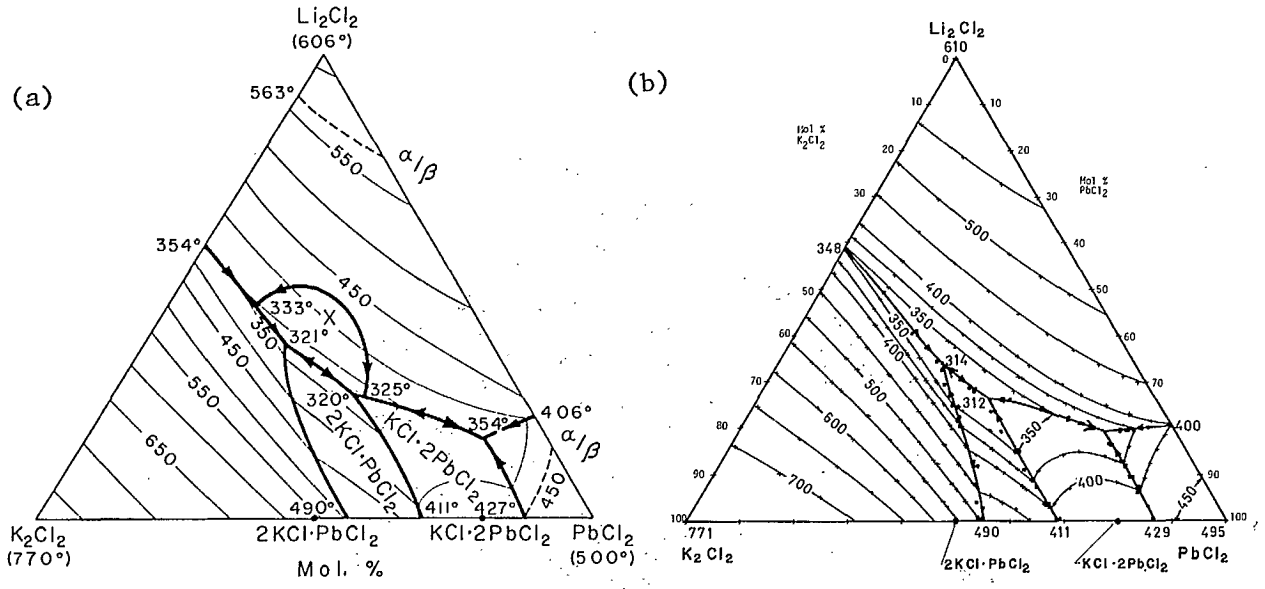

FIG. 3254.—System KCl-LiCl-$PbCl_2$. X represents an incongruently melting ternary compound of undetermined composition.

A. G. Bergman, Yu. I. Andryushchenko, and R. K. Bineeva, *Zh. Neorgan. Khim.*, 8 [7] 1693 (1963); *Russ. J. Inorg. Chem.* (*English Transl.*), 881 (1963).

Fig. 6 - (a) Measured (6b) and (b) calculated (this work) phase diagrams of the LiCl-KCl-$PbCl_2$ system

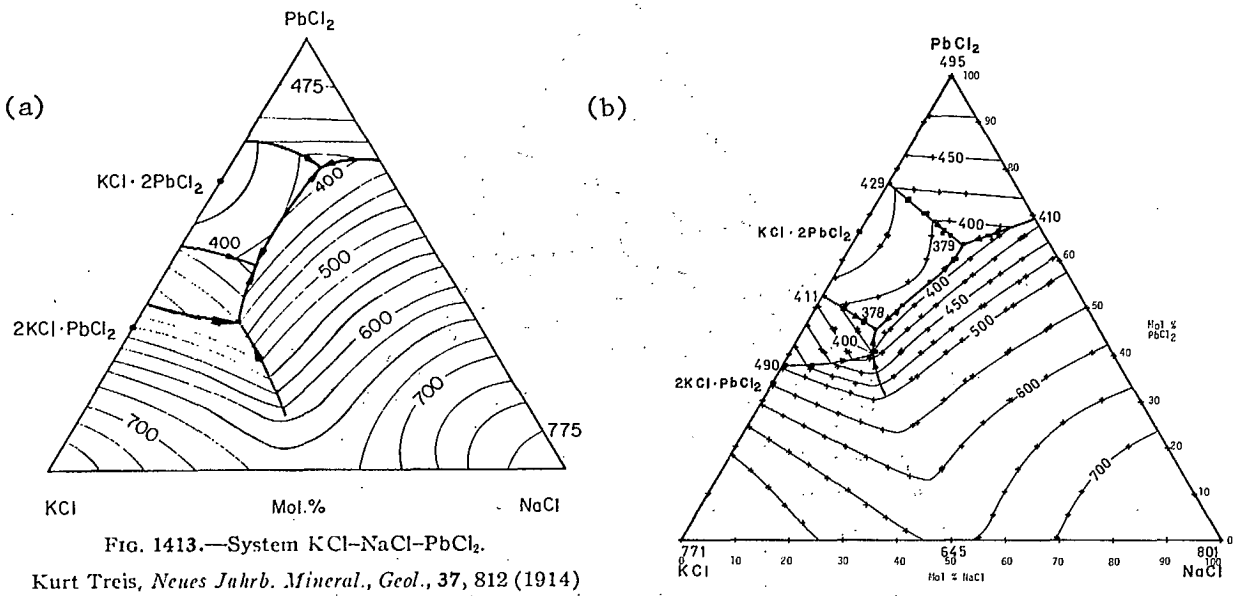

FIG. 1413.—System KCl-NaCl-$PbCl_2$.

Kurt Treis, *Neues Jahrb. Mineral., Geol.*, 37, 812 (1914)

Fig. 7 - (a) Measured (6a) and (b) calculated (this work) phase diagrams of the NaCl-KCl-$PbCl_2$ sytstem

(which will tend to occur at the lowest temperatures within the ternary regions) in Fig. 2-5, find the probable maximum error of each of the three binary sub-systems as listed in the previous section, take the largest of these, and multiply by 2.

For the four ternary systems, isothermal sections at several temperatures were calculated. These are given in Appendix B. (For identification of the phases, refer to the polythermal projections of Fig. 2-5). All compositions are in mole percentages.

ISO-ACTIVITY, ISO-VAPOUR PRESSURE AND ISO-DECOMPOSITION POTENTIALS

Computer generated iso-activity curves (with respect to the liquid standard state) of the components $PbCl_2$ and $ZnCl_2$ in the ternary systems are given in Appendix C at the temperatures specified. Compositions of all these diagrams are given in mole percentages. Note that some of the low temperature iso-activity lines represent activities in a metastable liquid below the liquidus surface.

Probable maximum error in the reported activities is about ± 20% in log a. Hence, if the activity is reported as a = 0.5, then log a is -0.30 ± 20% (of -0.30), which corresponds to a = $0.50^{\times}_{\div}$ (multiplied or divided by) 0.87.

Each iso-activity curve is also an iso-vapour pressure line, in which P_i, the vapour pressure of component i, is related to a_i, the activity of component i, by the equation

$$P_i = a_i . P_i^o \qquad \text{Eq 10}$$

where P_i^o is the vapour pressure of pure i at the temperature in question. Equation 10 is valid, however, only if i exists in the gas phase as molecules of i, and not as dimers, etc. That is, for $ZnCl_2$, we can write $P_{ZnCl_2} = a_{ZnCl_2} . P^o_{ZnCl_2}$ only if $ZnCl_2$ molecules exist in the gas phase. If there are Zn_2Cl_4 dimerized gas molecules, for instance, or if there is a reaction with other components so as to give gaseous molecules such as $LiZnCl_3$, for example, then Eq 10 no longer holds. For the components $ZnCl_2$ and $PbCl_2$, experimental evidence (14,15) indicates that only $ZnCl_2$ and $PbCl_2$ gas molecules exist in appreciable quantities at the temperatures and pressures of interest here.

Vapour pressures of the pure chlorides, P_i^o, calculated from data in the literature (4) are listed in Table 3. Errors in log P_i^o are expected to be of the order of ± 5% or less. Thus if $P_i^o = 10^{-3}$ atm, then log P_i^o = - 3.00 ± 0.15, and if log a_i = - 0.30 ± 0.06 (as above), then log P_i = -3.30 ± 0.21 or $P_i = 5.01 \times 10^{-4}$ atm ($\overset{\times}{\div}$ 1.62).

The iso-activity lines are also lines of iso-decomposition potential, ε_i. For $PbCl_2$ and $ZnCl_2$, ε_i is given in mV as:

$$\varepsilon_{ZnCl_2} = \varepsilon^o_{ZnCl_2} - 0.04308 T \ln a_{ZnCl_2} \ (mV) \qquad \text{Eq 12}$$

where $\varepsilon^o_{PbCl_2}$ and $\varepsilon^o_{ZnCl_2}$ are the standard decomposition potentials of liquid $PbCl_2$ and $ZnCl_2$ at T,K. Values calculated from tabulated thermodynamic data (4) are listed for the required temperatures in Table 4. Errors in $\varepsilon^o_{PbCl_2}$ and $\varepsilon^o_{ZnCl_2}$ are estimated as ± 5% or less.

SELECTION OF SUITABLE ELECTROLYTE TEMPERATURES AND COMPOSITIONS FOR LEAD AND ZINC ELECTROWINNING

In the following discussion of ternary systems of the type ACl-BCl-MCl_2 (where A and B are alkali metal cations and M = Pb or Zn), the fraction of the total amount of alkali chloride which is ACl is given by:

$$t = \frac{\text{mol \% ACl}}{\text{mol \% ACl + mol \% BCl}} \qquad \text{Eq 13}$$

The concentration of MCl_2 is simply expressed in mole per cent. The concentrations of the alkali chlorides are then given by:

$$\text{mol \% ACl} = t(100 - \text{mol \% } MCl_2) \qquad \text{Eq 14}$$

$$\text{mol \% BCl} = (1-t)(100 - \text{mol \% } MCl_2) \qquad \text{Eq 15}$$

Table 3 - Vapour pressures of pure chlorides P^o (atm) (4)

T(°C)	$PbCl_2$	$ZnCl_2$
300	0.84×10^{-7}	
325	0.33×10^{-6}	
350	0.12×10^{-5}	
375	0.37×10^{-5}	
400	0.11×10^{-4}	0.563×10^{-3}
425	0.28×10^{-4}	0.131×10^{-2}
450	0.68×10^{-4}	0.286×10^{-2}
475	0.157×10^{-3}	0.589×10^{-2}
500	0.340×10^{-3}	0.0115
525	0.697×10^{-3}	0.0215
550	0.136×10^{-2}	0.0385
575	0.254×10^{-2}	0.0662
600	0.456×10^{-2}	0.110
625	0.788×10^{-2}	0.177
650	0.0132	0.277
675	0.0213	0.421
700	0.0335	0.624
750		1.29

Table 4 - Standard decomposition potentials of $PbCl_2$ and $ZnCl_2$ liquid (4)

T(°C)	$\varepsilon^o_{PbCl_2}$ (mV)	$\varepsilon^o_{ZnCl_2}$ (mV)
300	1140	
325	1380	
350	1370	
375	1350	
400	1330	1630
425	1320	1610
450	1300	1590
475	1290	1580
500	1280	1560
525	1260	1540
550	1250	1520
575	1230	1510
600	1220	1490
625	1200	1470
650	1190	1460
675	1180	1440
700	1160	1420
750		1390

Thus in the LiCl-KCl-$PbCl_2$ system, if ACl = LiCl and BCl = KCl, then t = 1.0 for the LiCl-$PbCl_2$ binary system and t = 0.0 for the KCl-$PbCl_2$ system. In Fig. 8, for example, the value of t at point A is 0.32 (as seen from the projection to point B) while the concentration of $PbCl_2$ is 36 mol % (point C). Hence the concentrations of LiCl and KCl are 43.5 and 20.5 mol % respectively. This method of describing compositions in these systems is more appropriate than that which gives the concentrations of each of the three components individually, since the concentration of MCl_2 will vary to a greater or lesser extent along lines of constant values of t during electrolysis, while the amounts of ACl and BCl will remain constant.

To establish temperatures and compositions suitable from a thermodynamic viewpoint for electrowinning of lead and zinc, selected isothermal phase equilibria sections and ternary iso-activity sections from Appendices II and III were combined to produce Fig. 8 to 25. The lines which define the irregularly shaped areas within the composition triangles of Fig. 8 to 25 represent compositions of solid-liquid equilibria. Within these areas, which represent compositions of one-phase liquid solutions, are shown iso-vapour pressure lines of MCl_2 calculated by the method described in the previous section. Vapour pressures are given in units of torr throughout this report as these units are used more extensively than the pascal (Pa), which is the SI unit for pressure (see, for example, reference 4). (The conversion factor is 1 torr = 1 mm Hg = 1.333224×10^2 Pa).

Although the volatility of a component of a fused salt solution depends on its vapour pressure, the geometry of the enclosure and the turbulence of the surrounding or imposed atmosphere, volatilization of the base metal chlorides is not expected to lead to significant electrolyte losses if their vapour pressures are less than 0.1 torr.

The concentrations of MCl_2 suitable for electrowinning at various temperatures have been determined within these areas of one-phase liquid solution to ensure that no solid phases precipitate in the electrolytes, and by taking into account the maximum probable errors associated with

each calculated system. These concentrations are based on thermodynamic considerations only and may in fact be unsuitable with respect to electrolyte viscosity, conductivity, stability in the presence of air and kinetic considerations.

The discussions which follow apply to the systems at constant temperature. Temperature gradients within the molten salts could cause the formation of solid phases and interfere with electrolysis.

ELECTROWINNING OF LEAD

LiCl-KCl-$PbCl_2$

With this system as an electrolyte, the minimum temperature suitable for lead electrowinning is approximately 375°C, as seen from Fig. 8 to 12. At 350°C, Fig. 8, the composition range of one-phase liquid solution is likely too small to be suitable for electrowinning. At 375°C, however, for concentrations of $PbCl_2$ between 15 and 40 mol %, a corridor of miscibility exists centred around $t \simeq 0.55$ as shown in Fig. 9. Electrolyte depletion of $PbCl_2$ within these limits will not cause the formation of a solid phase. At 40 mol % $PbCl_2$, t could be varied between 0.30 and 0.56 to obtain desired electrolyte properties. The maximum $PbCl_2$ concentrations in this and in the NaCl-KCl-$PbCl_2$ systems are given in Table 5 along with the corresponding vapour pressures, decomposition potentials and ranges of t.

At 40 mol % $PbCl_2$ concentration and 375°C, the minimum partial pressure of $PbCl_2$ is calculated to be 0.0006 torr ($\overset{x}{\div}$ 2.57). While this is probably not enough to volatilize significant quantities of $PbCl_2$, collection systems would most likely be required to maintain the airborne quantities of $PbCl_2$, which are calculated to be $\simeq$ 30 mg/m^3, within health standard limits, which will be reduced in the United States from the present 200 $\mu g/m^3$ to 100 $\mu G/m^3$ in 1983.

An increase in temperature to 400°C increases the maximum concentration of $PbCl_2$ to 60 mol %, as shown in Fig. 10, and also increases P_{PbCl_2} to 0.004 torr ($\overset{x}{\div}$ 2.0). At 450°C, Fig. 11, the maximum concentration of $PbCl_2$ is 75 mol % for $0.00 \leq t \leq 1.00$, and P_{PbCl_2} increases to 0.036 torr ($\overset{x}{\div}$ 1.74). At higher temperatures, say 500°C (Fig. 12), the maximum concentration of $PbCl_2$ can be expected to be set by electrolyte properties, rather than phase boundary limitations, since $PbCl_2$ melts at 495°C.

From the foregoing, it can be seen that both the temperature and composition of the system LiCl-KCl-$PbCl_2$ may be varied widely to determine suitable properties of density, conductivity and viscosity for electrolysis.

NaCl-KCl-$PbCl_2$

Reference to Fig. 13 to 17 indicates that the minimum temperature at which a significant field of one-phase liquid solution exists in this

Table 5 - Maximum concentrations of $PbCl_2$ in possible fused ternary chloride electrolytes

System	T(°C)	Maximum $PbCl_2$ concentration, mol %	Range of t* at maximum $PbCl_2$ concentration	P_{PbCl_2}, torr	$\varepsilon^o_{PbCl_2}$, mV	ε_{PbCl_2}, mV
LiCl-KCl-$PbCl_2$	375	40	0.30 - 0.56	0.0008 ($\overset{x}{\div}$ 2.38) to 0.0006 ($\overset{x}{\div}$ 2.57)	1350	1385
(A=Li, B=K)						
	400	60	0.20 - 0.50	0.004 ($\overset{x}{\div}$ 2.03)	1330	1350
	425	70	0.00 - 0.70	0.13 ($\overset{x}{\div}$ 1.87)	1320	1330
	450	75	0.00 - 1.00	0.36 ($\overset{x}{\div}$ 1.74)	1300	1305
NaCl-KCl-$PbCl_2$	425	70	0.32 - 1.00	0.013 ($\overset{x}{\div}$ 1.87)	1320	1335
(A=Na, B=K)	450	75	0.00 - 1.00	0.04 ($\overset{x}{\div}$ 1.74)	1300	1310

* $t = \frac{\text{mol \% ACl}}{\text{mol \% ACl + mol \% BCl}}$

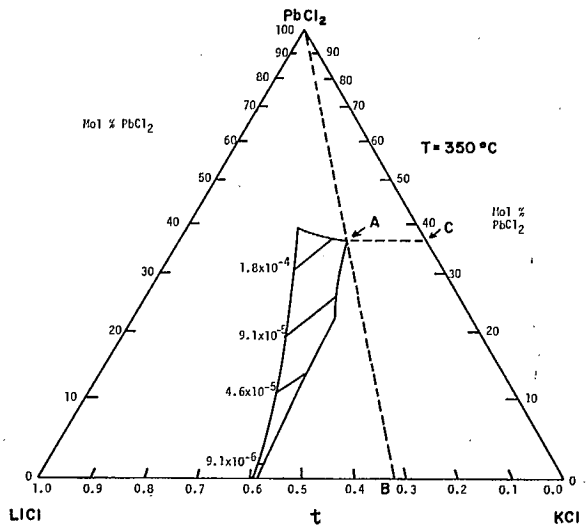

Fig. 8

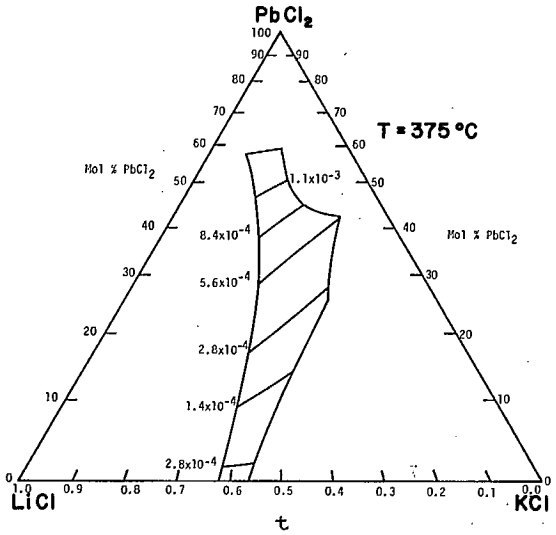

Fig. 9

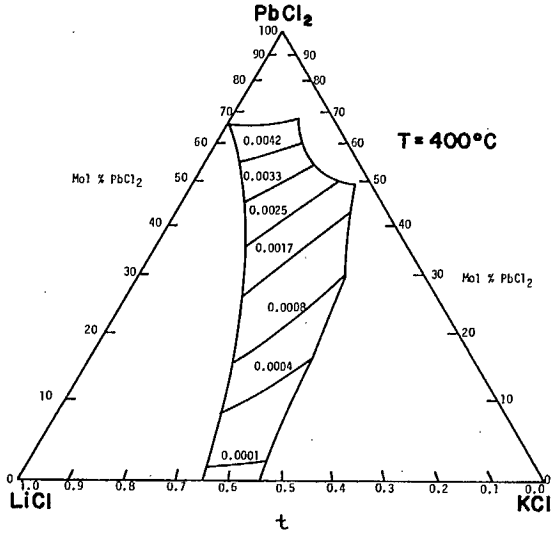

Fig. 10

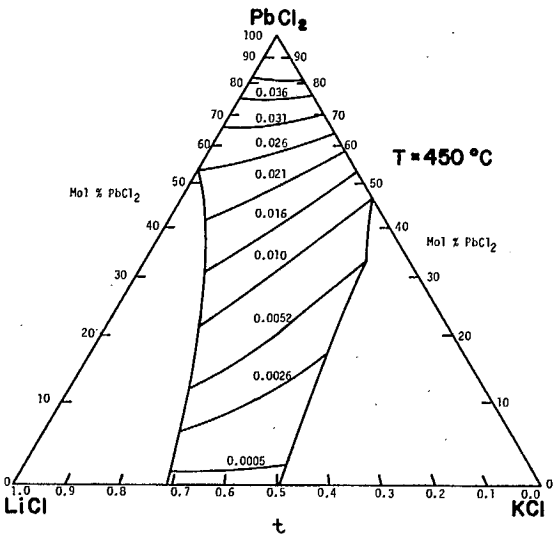

Fig. 11

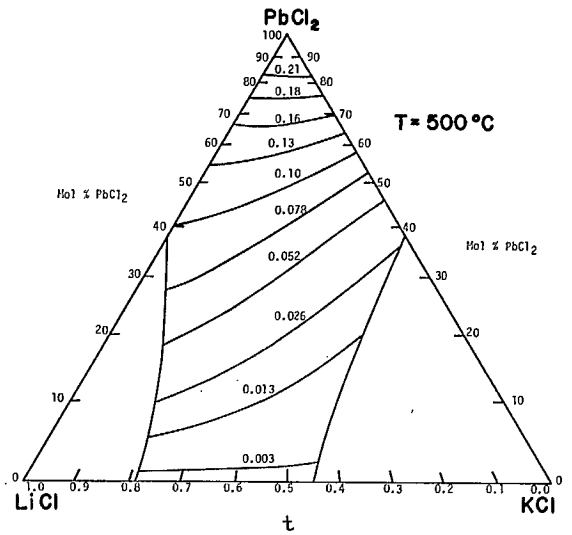

Fig. 12

Fig. 8, 9, 10, 11, 12 - Iso-vapour pressure lines of $PbCl_2$ and the composition region of one-phase liquid solution in the system LiCl-KCl-$PbCl_2$ at temperatures from 350-500°C. The units of the iso-vapour pressure lines are torr (mm Hg).

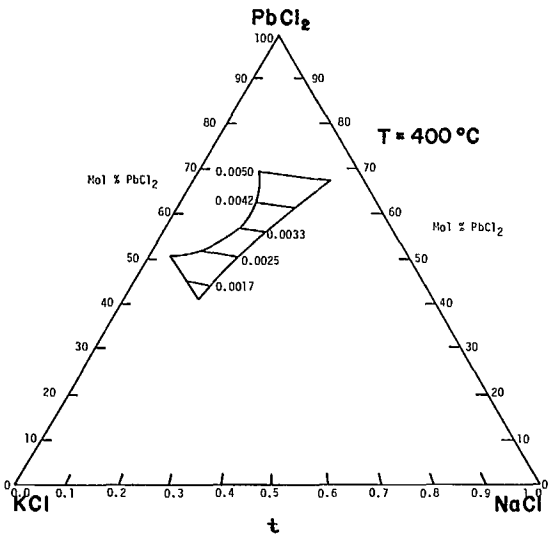

Fig. 13

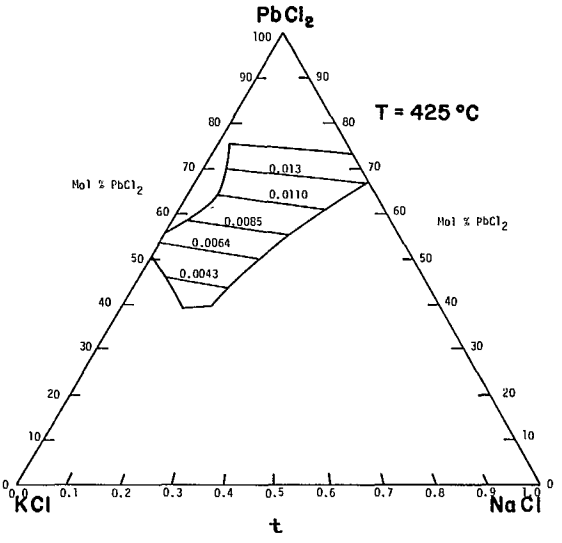

Fig. 14

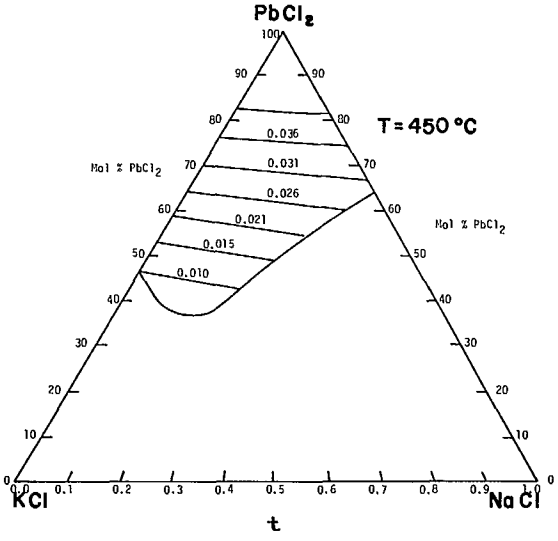

Fig. 15

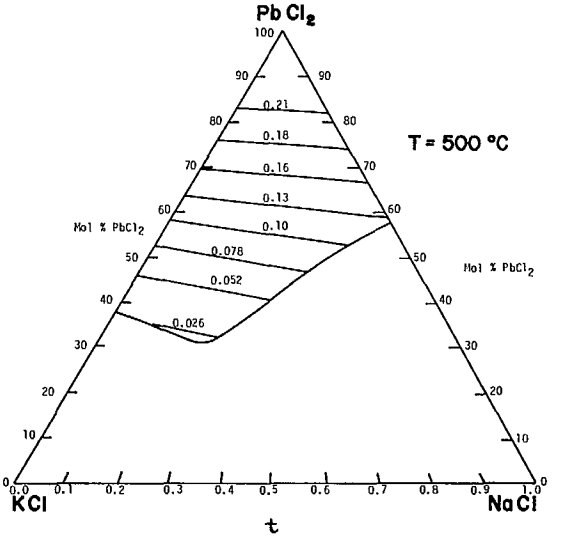

Fig. 16

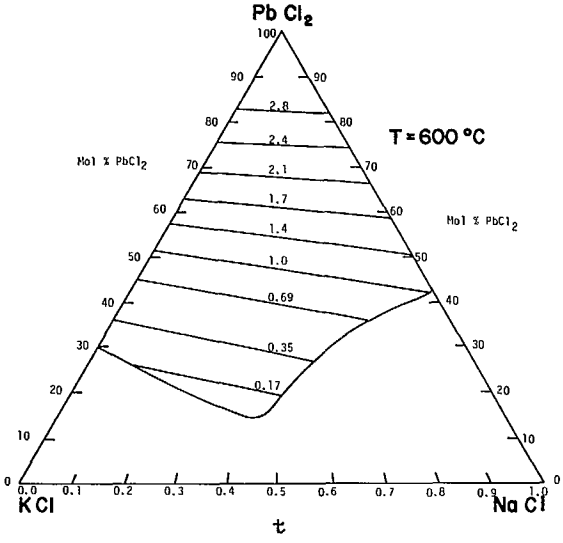

Fig. 17

Fig. 13, 14, 15, 16, 17 - Iso-vapour pressure lines of $PbCl_2$ and the composition region of one-phase liquid solution in the system NaCl-KCl-$PbCl_2$ at temperatures from 400-600°C. The units of the iso-vapour pressure lines are torr (mm Hg).

system is 425°C. At this temperature, as seen in Fig. 14, the maximum concentration of $PbCl_2$ is 70 mol %, for which t can vary between 0.32 and 1.00 with little effect on vapour pressure which remains at ≃ 0.013 torr ($\overset{x}{\div}$ 1.87). At 450°C, Fig. 15, the maximum suitable concentration of $PbCl_2$ increases to 75 mol %, accompanied by an increase in P_{PbCl_2} to ≃ 0.04 torr ($\overset{x}{\div}$ 1.74), at which pressure significant volatilization of $PbCl_2$ would not occur. As with $LiCl-KCl-PbCl_2$, the maximum concentration of $PbCl_2$ at temperatures higher than 450°C will be set by electrolyte properties rather than phase limitations. However, unlike $LiCl-KCl-PbCl_2$, this system does not have a wide range of temperatures below 495°C over which significant regions of liquid miscibility exist.

The decomposition potentials, ε_{PbCl_2}, for $PbCl_2$ in both fused salt systems are only 10-40 mv greater than the standard decomposition potentials of $PbCl_2$, $\varepsilon°_{PbCl_2}$, at each temperature. This is because no significant reduction in a_{PbCl_2} below ideality occurs in the concentration ranges under consideration.

ELECTROWINNING OF ZINC

For the $LiCl-KCl-ZnCl_2$ and the $NaCl-KCl-ZnCl_2$ fused salt systems, the lower temperature limit for electrolysis is set by the melting point of zinc, 420°C, rather than the melting point of the electrolyte as with $PbCl_2$ systems. As $ZnCl_2$ is molten at 318°C and high concentrations of $ZnCl_2$ cause low current efficiencies as well as high decomposition potentials during electrolysis (13), it is more appropriate in this case to determine the minimum rather than the maximum concentration of $ZnCl_2$ for which one-phase liquid solutions exist.

$LiCl-KCl-ZnCl_2$

In this system there are ranges of minimum concentrations of $ZnCl_2$ which correspond to compositions along various iso-vapour pressure lines as seen in Fig. 18 to 20. The minimum $ZnCl_2$ concentrations in this and in the $NaCl-KCl-ZnCl_2$ systems are given in Table 6 along with the corresponding vapour pressures and decomposition potentials. As seen in Fig. 18, the concentration P_{ZnCl_2} = 0.0011 torr ($\overset{x}{\div}$ 6.13). However, once t exceeds 0.35, it would be necessary to maintain the concentration of $ZnCl_2$ within ± 5 mol % to prevent the formation of a solid phase. At 500°C, Fig. 19, the minimum $ZnCl_2$ composition range is similar to that of 450°C while P_{ZnCl_2} has increased to 0.004 torr ($\overset{x}{\div}$ 5.72). However, maintaining the concentration of $ZnCl_2$ within narrow limits is not necessary at this temperature because of the wider range of one-phase liquid solution than at 450°C.

At 550°C, Fig. 20, the region of one-phase liquid solution encompasses most of this isothermal section of the phase diagram. The minimum concentration range of $ZnCl_2$ is similar to those at lower temperatures but t can vary between 0.00 and 0.80. The corresponding values of P_{ZnCl_2} are 0.015 torr ($\overset{x}{\div}$ 5.38) and 0.15 torr ($\overset{x}{\div}$ 3.40). Of the pressures at which the concentration of $ZnCl_2$ is a minimum in this system, the latter is the only one at which significant volatilization of $ZnCl_2$ could occur. Increasing the concentration of $ZnCl_2$ at a constant value of t will of course increase P_{ZnCl_2}.

$NaCl-KCl-ZnCl_2$

In this system, the minimum concentration of $ZnCl_2$ at 450°C, as shown in Fig. 21, is 40 mol % for which $0.00 \leq t \leq 0.08$ and P_{ZnCl_2} = 0.022 torr ($\overset{x}{\div}$ 3.37). At 40 mol % $ZnCl_2$, an increase in the concentration of NaCl such that t becomes greater than 0.08 would, to avoid the formation of a solid phase, necessitate increasing the concentration of $ZnCl_2$ to approximately 47 mol % at which P_{ZnCl_2} = 0.33 torr ($\overset{x}{\div}$ 1.95) for t = 0.50. At 500°C, as seen in Fig. 22, the minimum concentration of $ZnCl_2$ is reduced to 30 mol % for which $0.00 \leq t \leq 0.10$ and P_{ZnCl_2} ≃ 0.005 torr ($\overset{x}{\div}$ 3.6). An increase in NaCl concentration at this temperature increases the minimum concentration of $ZnCl_2$ to ≃ 43 mol % at which P_{ZnCl_2} ≃ 1.1 torr ($\overset{x}{\div}$ 1.9) for t = 0.50. At this pressure $ZnCl_2$ vapour losses would be significant.

The more extensive regions of one-phase liquid solution obtained on increasing temperature enable the reduction of the minimum concentration of $ZnCl_2$ to such an extent that, for low values of

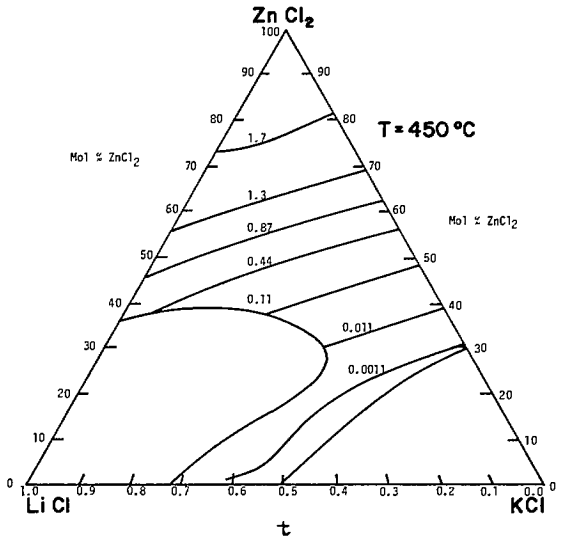

Fig. 18

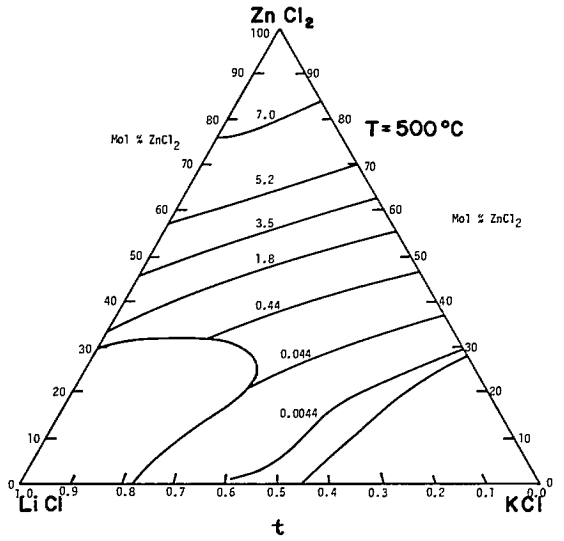

Fig. 19

Fig. 18, 19, 20 - Iso-vapour pressure lines of $ZnCl_2$ and the composition region of one-phase liquid solution in the system LiCl-KCl-$ZnCl_2$ at temperatures from 450-550°C. The units of the iso-vapour pressure lines are torr (mm Hg).

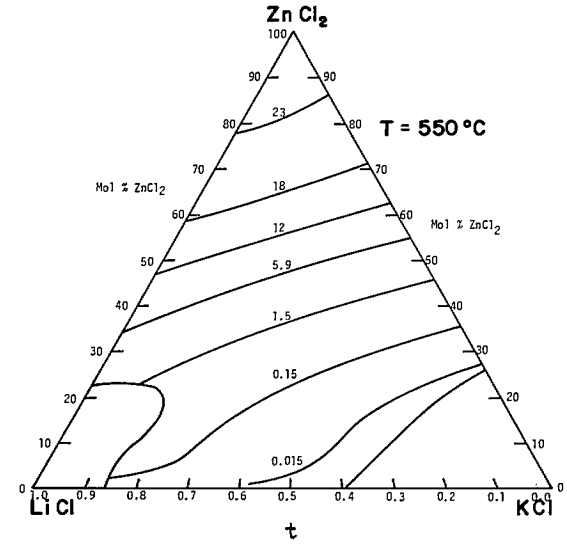

Fig. 20

t, the reduced activity of $ZnCl_2$ compensates for the two order of magnitude increase in $P^o_{ZnCl_2}$ between 450°C and 650°C (0.286 x 10^{-2} to 0.277 atm), so that the minimum P_{ZnCl_2} remains below 0.05 torr, at which pressure significant volatilization of $ZnCl_2$ would not be possible up to 650°C. However, for t = 0.50, P_{ZnCl_2} increases from 0.33 torr at 450°C to 2.0 torr at 650°C, and at these pressures one could expect some volatilization of $ZnCl_2$. These data are shown in Fig. 21 to 25 and are given in Table 6.

Because the concentrations of $ZnCl_2$ under consideration are lower than the concentrations of $PbCl_2$ previously discussed, but more importantly because of the reduced activity of $ZnCl_2$ due to complex anion formation (9), the decomposition potentials, ε_{ZnCl_2}, for $ZnCl_2$ in both ternary fused chloride systems are between 140 and 365 mv greater than the standard decomposition potentials, $\varepsilon^o_{ZnCl_2}$. This is indicated in Table 6.

The data of Fig. 18-25 in general indicate that, to the extent permitted by phase limitations, KCl-rich regions of the $ZnCl_2$ systems can be enriched in LiCl or NaCl to enhance electrolyte properties (such as conductivity and viscosity) without increasing P_{ZnCl_2}.

CONCLUSIONS

Phase diagrams and base metal chloride iso-activity curves in the ternary fused salt systems LiCl-KCl-$PbCl_2$, NaCl-KCl-$PbCl_2$, LiCl-KCl-$ZnCl_2$ and NaCl-KCl-$ZnCl_2$ have been calculated by means of analytical techniques from the known thermodynamic properties of the appropriate binary systems. For the two ternary systems involving $PbCl_2$, the calculated and experimentally measured phase diagrams were in agreement within experimental error. For the two ternary systems involving $ZnCl_2$, it is believed that the measured phase diagrams are in such serious error that the calculated phase diagrams are to be preferred.

Isothermal phase sections of the calculated phase diagrams were then combined with base metal chloride iso-vapour pressure curves (calculated in turn from the iso-activity curves) to determine ranges of temperature and composition in which a one-phase liquid electrolyte would be

Table 6 - Minimum concentrations of $ZnCl_2$ in possible ternary fused chloride electrolytes

System	T(°C)	Minimum $ZnCl_2$ concentration, mol %	Range of t* at minimum $ZnCl_2$ concentration	P_{ZnCl_2}, torr	$\varepsilon^o_{ZnCl_2}$, mV	ε_{ZnCl_2}, mV
LiCl-KCl-$ZnCl_2$	450	30-0	0.00 - 0.60	0.001 ($\frac{x}{\div}$ 6.13)	1590	1830
(A=Li, B=K)	500	30-0	0.00 - 0.60	0.004 ($\frac{x}{\div}$ 5.72)	1560	1810
	550	30-0	0.00 - 0.75	0.015 ($\frac{x}{\div}$ 5.38) to 0.15 ($\frac{x}{\div}$ 3.40)	1520	1780
NaCl-KCl-$ZnCl_2$	450	35	0.00 - 0.08	0.022 ($\frac{x}{\div}$ 3.37)	1590	1730
(A=Na, B=K)		47	0.50	0.33 ($\frac{x}{\div}$ 1.95)		
	500	30	0.00 - 0.10	0.005 ($\frac{x}{\div}$ 3.61)	1560	1740
		43	0.50	1.1 ($\frac{x}{\div}$ 1.9)		
	550	26	0.00 - 0.15	0.029 ($\frac{x}{\div}$ 5.38)	1520	1790
		38	0.50	1.5 ($\frac{x}{\div}$ 2.1)		
	600	25-20	0.00 - 0.33	0.042 ($\frac{x}{\div}$ 5.11)	1490	1780
				2.0 ($\frac{x}{\div}$ 2.35)		
	650	22-0	0.00 - 0.50	0.021 ($\frac{x}{\div}$ 6.73)	1460	1830

* $t = \frac{\text{mol \% ACl}}{\text{mol \% ACl + mol \% BCl}}$

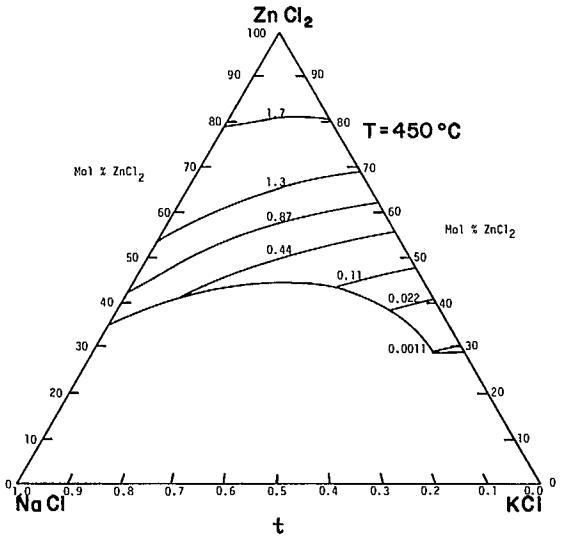

Fig. 21

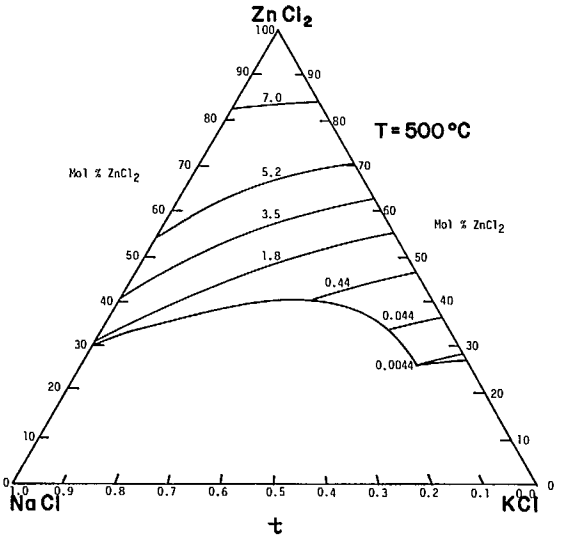

Fig. 22

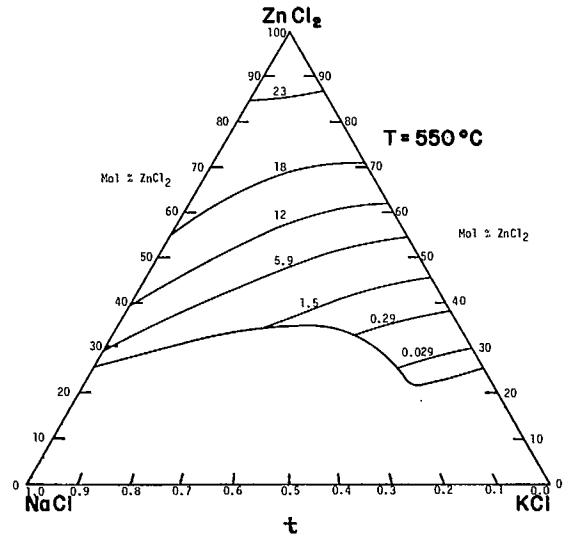

Fig. 23

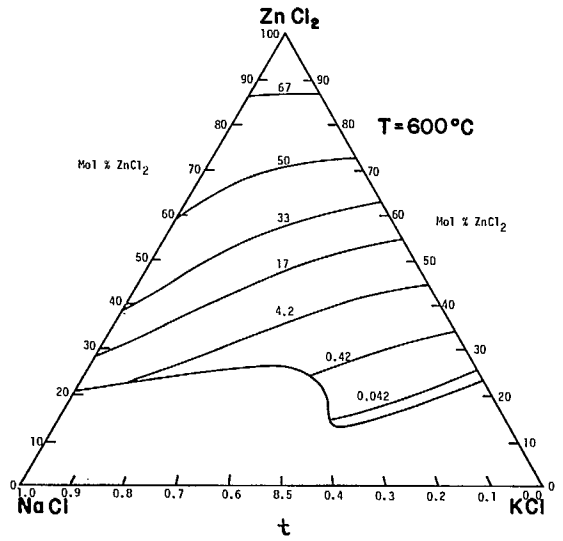

Fig. 24

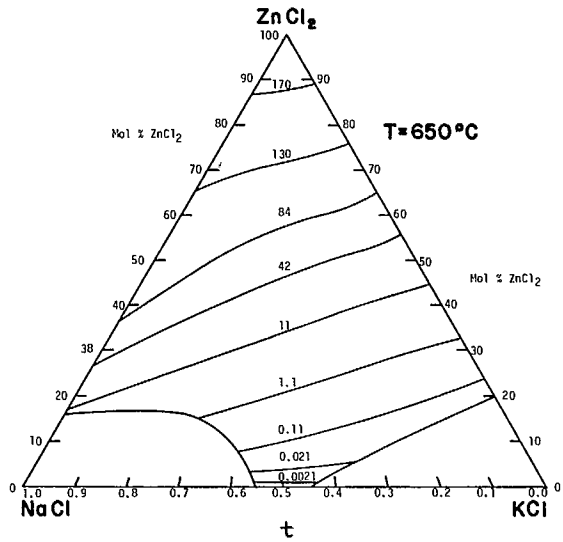

Fig. 25

Fig. 21, 22, 23, 24, 25 - Iso-vapour pressure lines of $ZnCl_2$ and the composition region of one-phase liquid solution in the system NaCl-KCl-$ZnCl_2$ at temperatures from 450-650°C. The units of the iso-vapour pressure lines are torr (mm Hg).

maintained and in which the vapour pressure of the base metal chloride would be less than 0.1 torr, i.e. low enough to prevent its significant volatilization. Each of the four systems has wide ranges of temperature and composition exhibiting a one-phase liquid solution over which the vapour pressure of the metal chloride is less than 0.1 torr.

Within each region of one-phase liquid solution, extensive variations of density, viscosity and electrical conductivity can be expected to occur. The experimental measurement of these intensive properties, combined with the thermodynamic properties given in this report, will enable a determination of the optimum temperature and composition for each of the four ternary systems. Hence, future investigation into these systems could involve the measurement of the density, viscosity and conductivity of their regions of one-phase liquid solution as well as the experimental verification of some of the calculated vapour pressures in the $PbCl_2$ and $ZnCl_2$ systems and of the $ZnCl_2$ ternary phase diagrams.

REFERENCES

1. Lin, P.-L., Pelton, A.D. and Bale, C.W. J Am Ceram Soc 62:414; 1979.

2. Saboungi, M.L., Lin, P.-L., Cerisier, P. and Pelton, A.D. Met Trans B in press.

3. Liang, W.W., Lin, P.-L. and Pelton, A.D., High Temp Sci 12:41; 1980.

4. Barin, I., Knacke, O. and Kubaschewski, O. "Thermochemical Properties of Inorganic Substances"; Springer-Verlag, N.Y. 1973 and Supplement (1977).

5. Pelton, A.D. and Bale, C.W. CALPHAD Journal 1:253; 1977.

6a. Levin, E.M., Robbins, C.R. and McMurdie, H.F. "Phase Diagrams for Ceramists", The American Ceramic Society, Columbus, Ohio. U.S.A.; 1964.

6b. Levin, E.M., Robbins, C.R. and McMurdie, H.F., ibid., 1974 Supplement; 1975.

6c. Levin, E.M. and McMurdie, H.F., ibid., 1975 Supplement; 1975.

7. Hersh, L.S. and Kleppa, O.J. J Chem Phys 42: 1309; 1965.

8. McCarty, F.G. and Kleppa, O.J. J Phys Chem 68:3846; 1964.

9. Hagemark, K., Hengstenberg, D. and Blander, M. J Chem Eng Data 17:216; 1972.

10. Robinson, R.J. and Kucharski, A.S. Can J. Chem 51:3114; 1973.

11. Papatheodorou, G.N. and Kleppa, O.J. Z anorg allg Chem 10:132; 1973.

12. Janz, G.G. et al.; ACS Reprint No. 71(4), 1975.

13. Shanks, D.E., Haver, F.P., Elges, C.H. and Wong, M.M. U.S. Bureau of Mines, Report of Investigation 8343; 1979.

14. Hagemark, K., Hengstenberg, D. and Blander, M. J Phys Chem 71:1819; 1967.

15. Rice, D.W. and Gregory, N.W. J Phys Chem 72: 3361; 1968

APPENDIX A - BINARY SYSTEMS*

*Figure numbers on the diagrams in this section refer to the original diagrams from the three volumes of "Phase Diagrams for Ceramists".

Table A-1 Summary of optimized thermodynamic parameters

Binary System		Liquid Phase				Solid Solution Phase			Stoichiometric Solid Phases A_xB_{1-x}					
									$\Delta G^o_{fusion} = a + bT(\frac{cal}{mol})$			$\Delta G^o_{formation\ from\ pure\ liquids} = a' + b'T(\frac{cal}{mol})$		
A	B	i	j	enthalpy coeff., h_{ij} (cal)	excess entropy coeff., s_{ij} (cal/K)	i	j	enthalpy coeff., h_{ij} (cal)	x	a	b	x	a'	b'
KCl	LiCl	1	1	-4290	-0.6211									
		2	1	90	-0.6047									
KCl	NaCl	1	1	-490		1	1	2520						
		1	2	-65		1	2	800						
KCl	$PbCl_2$	1	1	-4130.6	-0.1832							2/3	-4202.0	2.6154
		2	1	75.1	0.7419							1/3	-5231.1	4.6067
		3	1	-4160.3	4.7726									
		4	1		-10.3336									
KCl	$ZnCl_2$	1	1	-8213.4	3.9419				2/3	2182.8	-3.0378	2/3	-7111.8	2.839
		1	2	-83715.4	-43.0026				3/5	12214.9	-23.1127	3/5	-17545.5	23.0239
		1	3	143627.5	50.3580				1/3	4481.3	-8.2563	1/3	-8115.6	7.5127
		1	4	-54557.4										
LiCl	$PbCl_2$	1	1	850	2.2870									
		2	1	700	-3.4416									
		3	1		2.4032									
LiCl	$ZnCl_2$	1	1	-760.4	-0.7524				2/3	3149.1	-4.9183	2/3	-3279.1	3.3166
		1	2	-5464.0	6.8056									
		1	3	21725.9										
		1	4	-11265.3										
NaCl	$PbCl_2$	1	1	-450	1.2855									
NaCl	$ZnCl_2$	1	1	-6881.0	3.9419				2/3	1820.2	-2.6399	2/3	-3734.6	2.4412
		1	2	-14981.5	-43.0026									
		1	3	29860.2	50.3580									
		1	4	-1556.2										

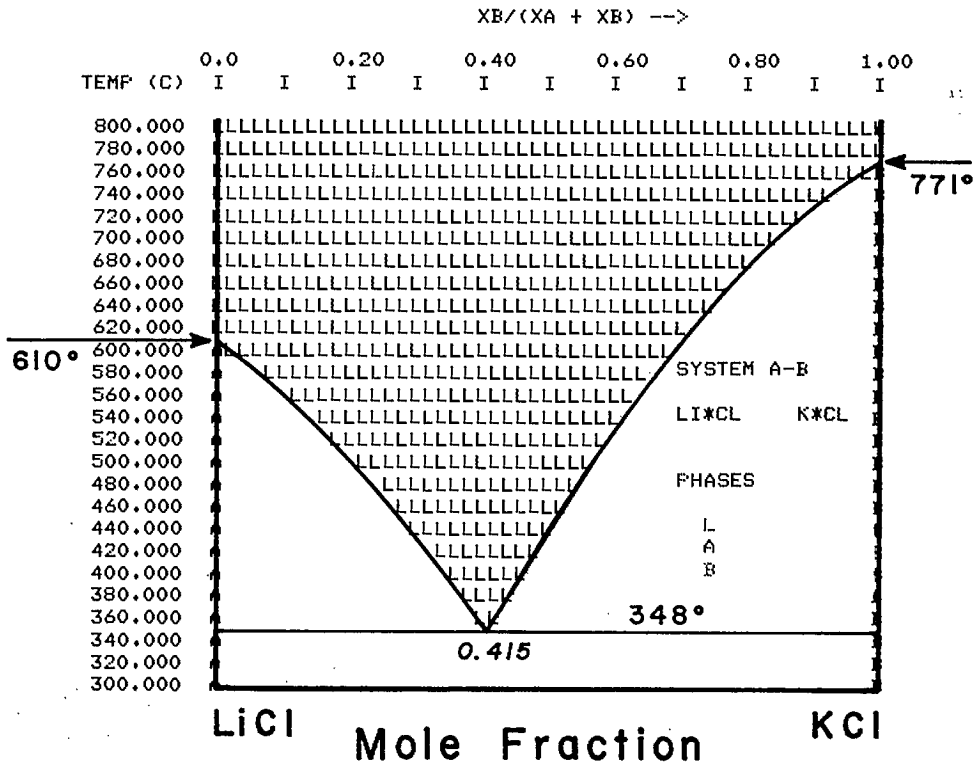

Fig. A-1 - Calculated and measured phase diagrams for LiCl-KCl

TEMP (C)	Compositions, in mole fractions, of phase boundaries			
800.000				
780.000				
760.000	0.97021	1.00000		
740.000	0.91943	1.00000		
720.000	0.87451	1.00000		
700.000	0.83350	1.00000		
680.000	0.79639	1.00000		
660.000	0.76221	1.00000		
640.000	0.73096	1.00000		
620.000	0.70068	1.00000		
600.000	0.0	0.02828	0.67334	1.00000
580.000	0.0	0.07645	0.64697	1.00000
560.000	0.0	0.11837	0.62158	1.00000
540.000	0.0	0.15454	0.59717	1.00000
520.000	0.0	0.18914	0.57471	1.00000
500.000	0.0	0.22096	0.55322	1.00000
480.000	0.0	0.25023	0.53271	1.00000
460.000	0.0	0.27861	0.51221	1.00000
440.000	0.0	0.30516	0.49365	1.00000
420.000	0.0	0.33081	0.47510	1.00000
400.000	0.0	0.35476	0.45752	1.00000
380.000	0.0	0.37893	0.43994	1.00000
360.000	0.0	0.40028	0.42432	1.00000
340.000	0.0	1.00000		
320.000	0.0	1.00000		
300.000	0.0	1.00000		

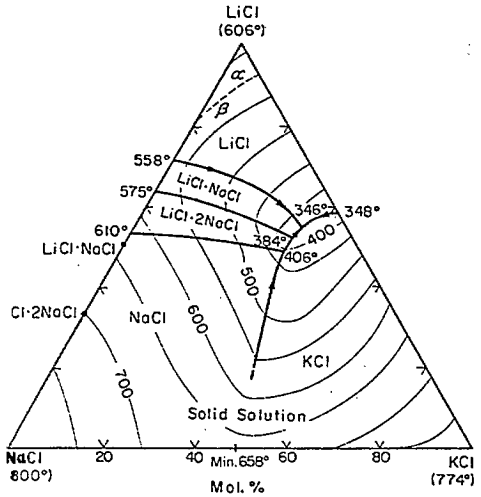

FIG. 3249.—System KCl–LiCl–NaCl.

E. K. Akopov and A. G. Bergman, *Zh. Neorgan. Khim.*, 11 1751 (1966); *Russ. J. Inorg. Chem.* (*English Transl.*), 938 (66).

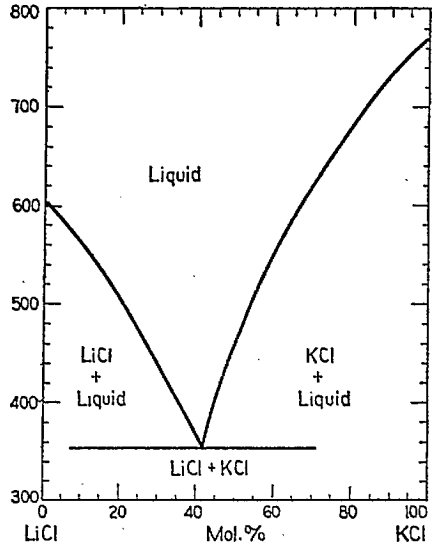

FIG. 1257.—System KCl–LiCl.

E. Elchardus and P. Laffitte, *Bull. soc. chim., France*, 51, 1572 (1932).

See also S. Zhemchuzhnui and F. Rambach, *Z. anorg Chem.*, 65, 406 (1910).

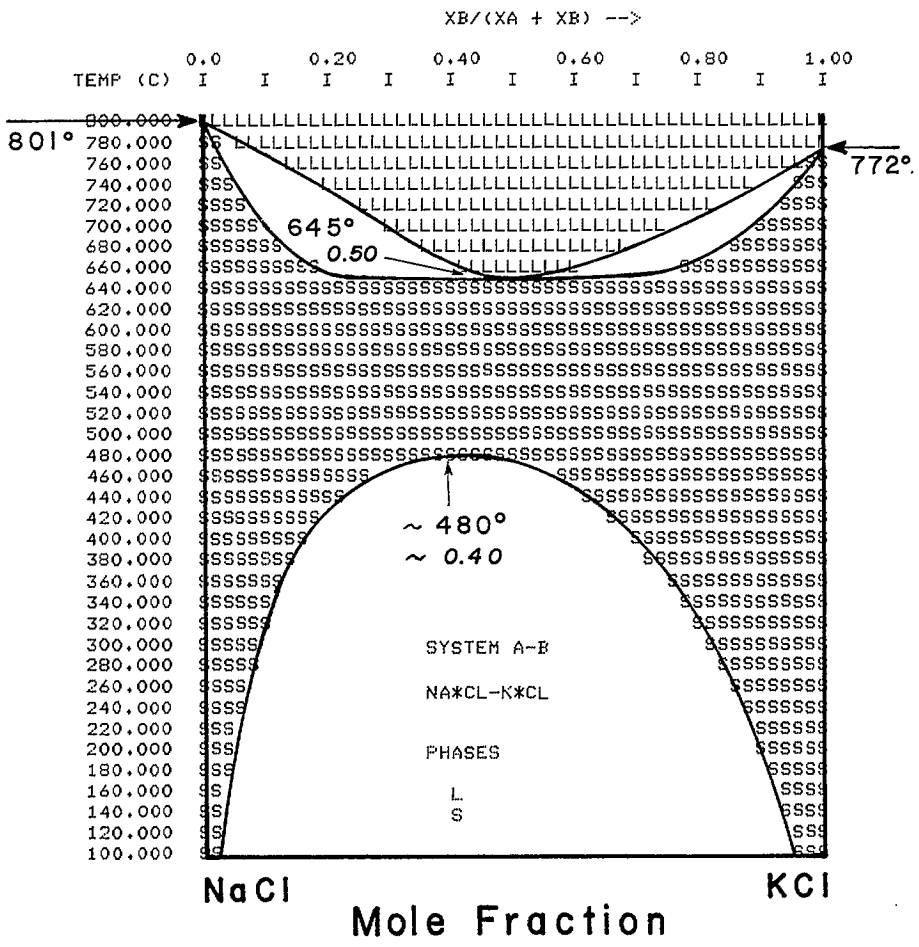

Fig. A-2 - Calculated and measured phase diagrams for NaCl-KCl

TEMP (C)	Compositions, in mole fractions of phase boundaries			
800.000	0.00049	0.00342		
780.000	0.01123	0.06982		
760.000	0.02490	0.13330	0.95850	0.98877
740.000	0.04053	0.19287	0.88525	0.96631
720.000	0.06006	0.25146	0.81299	0.93701
700.000	0.08545	0.30811	0.74365	0.90186
680.000	0.12158	0.36377	0.67334	0.85303
660.000	0.18604	0.42139	0.60010	0.77490
640.000				
620.000				
600.000				
580.000				
560.000				
540.000				
520.000				
500.000				
480.000				
460.000	0.25787	0.57281		
440.000	0.21891	0.62182		
420.000	0.18891	0.66166		
400.000	0.16393	0.69590		
380.000	0.14314	0.72613		
360.000	0.12479	0.75321		
340.000	0.10880	0.77851		
320.000	0.09480	0.80072		
300.000	0.08218	0.82214		
280.000	0.07101	0.84194		
260.000	0.06104	0.85977		
240.000	0.05205	0.87617		
220.000	0.04403	0.89149		
200.000	0.03700	0.90591		
180.000	0.03067	0.91872		
160.000	0.02508	0.93068		
140.000	0.02023	0.94135		
120.000	0.01620	0.95171		
100.000	0.01251	0.96011		

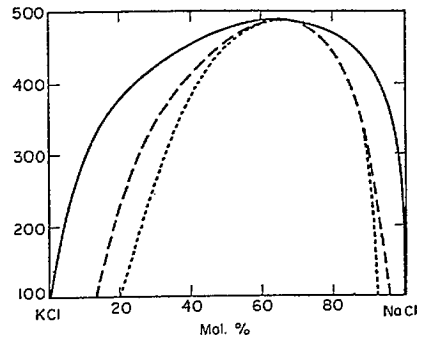

FIG. 1259.—System KCl–NaCl; solubility gap.

Solid line = experimental data; dashed line = spinodal curve; dotted curve = spinodal curve according to Erich Scheil and Hans Stadelmaier, *Z. Metallk.*, 43, 227 (1952). The limits of metastable equilibrium are defined by the solubility curve and the spinodal.

A. J. H. Bunk and G. W. Tichelaar, *Koninkl. Ned. Akad. Wetenschap. Proc. Ser. B*, 56, 378 (1953).

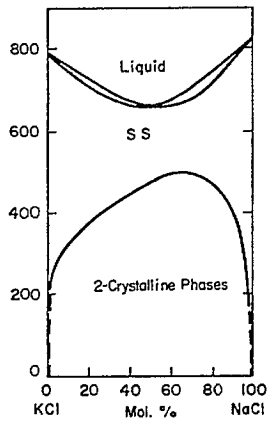

FIG. 1258.—System KCl–NaCl.

E. Scheil and H. Stadelmaier, *Z. Metallk.*, **43**, 227 (1952).

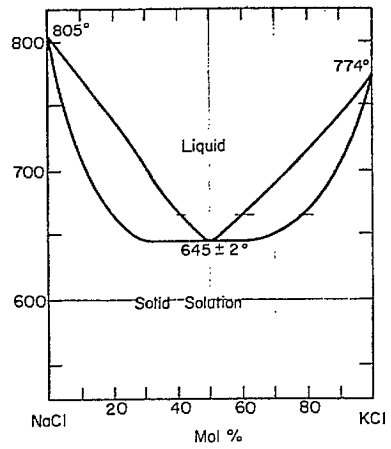

FIG. 4749.—System NaCl–KCl.

D. S. Coleman and P. D. A. Lacy, *Mater. Res. Bull.*, **2** [10] 936 (1967).

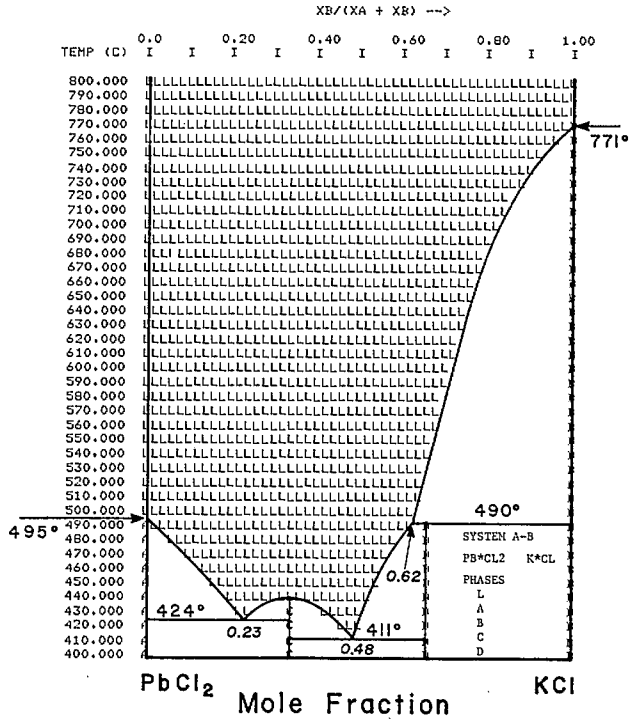

Fig. A-3 - Calculated and measured phase diagrams for KCl-$PbCl_2$

TEMP (C)	Compositions, in mole fractions, of phase boundaries									
800.000										
790.000										
780.000										
770.000	0.99756	1.00000								
760.000	0.96436	1.00000								
750.000	0.92822	1.00000								
740.000	0.89600	1.00000								
730.000	0.87061	1.00000								
720.000	0.84912	1.00000								
710.000	0.83154	1.00000								
700.000	0.81494	1.00000								
690.000	0.80029	1.00000								
680.000	0.78760	1.00000								
670.000	0.77490	1.00000								
660.000	0.76416	1.00000								
650.000	0.75244	1.00000								
640.000	0.74268	1.00000								
630.000	0.73291	1.00000								
620.000	0.72314	1.00000								
610.000	0.71436	1.00000								
600.000	0.70557	1.00000								
590.000	0.69678	1.00000								
580.000	0.68896	1.00000								
570.000	0.68018	1.00000								
560.000	0.67236	1.00000								
550.000	0.66455	1.00000								
540.000	0.65674	1.00000								
530.000	0.64990	1.00000								
520.000	0.64209	1.00000								
510.000	0.63525	1.00000								
500.000	0.62744	1.00000								
490.000	0.0	0.02458	0.61394	0.66667	0.66667	1.00000				
480.000	0.0	0.06473	0.58659	0.66667	0.66667	1.00000				
470.000	0.0	0.10221	0.56576	0.66667	0.66667	1.00000				
460.000	0.0	0.13742	0.54753	0.66667	0.66667	1.00000				
450.000	0.0	0.16882	0.53190	0.66667	0.66667	1.00000				
440.000	0.0	0.19864	0.51758	0.66667	0.66667	1.00000				
430.000	0.0	0.22597	0.24153	0.33333	0.33333	0.41896	0.50326	0.66667	0.66667	1.00000
420.000	0.0	0.33333	0.33333	0.45530	0.49024	0.66667	0.66667	1.00000		
410.000	0.0	0.33333	0.33333	0.66667	0.66667	1.00000				
400.000	0.0	0.33333	0.33333	0.66667	0.66667	1.00000				

KCl–$PbCl_2$

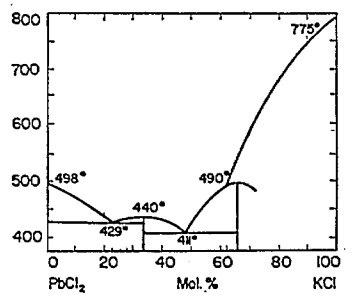

FIG. 1269.—System KCl–$PbCl_2$.

Ya A. Ugai and V. A. Shatillo, *J. Phys. Chem.* U.S.S.R., **23** [6] 745 (1949).

KCl–$PbCl_2$–KI–PbI_2

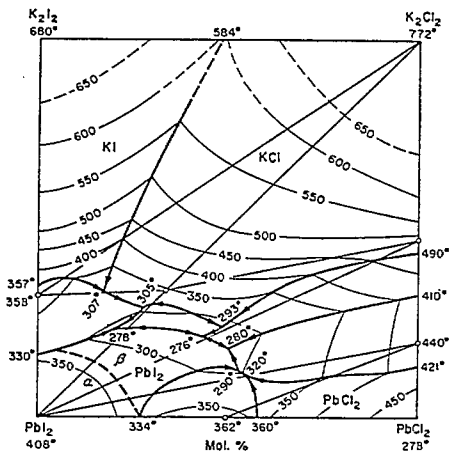

FIG. 1646.—System KCl–KI–$PbCl_2$–PbI_2; reciprocal.

I. I. Il'yasov and A. G. Bergman, *Zhur. Obshchei Khim.*, **26**, 987 (1956).

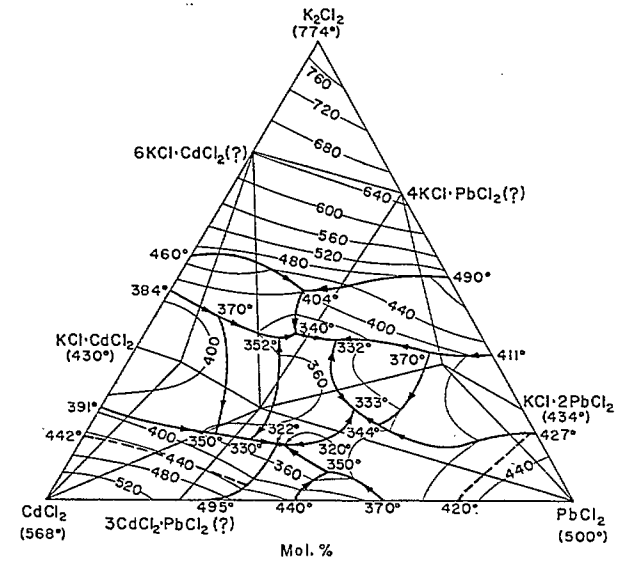

FIG. 3275.—System KCl–$CdCl_2$–$PbCl_2$. Triangulation of system is provisional as the compositions of the ternary compounds have not been established.

A. G. Bergman and Zh. V. Mishler, *Zh. Neorgan. Khim.*, 10 [5] 1282 (1965); *Russ. J. Inorg. Chem.* (*English Transl.*), 697 (1965).

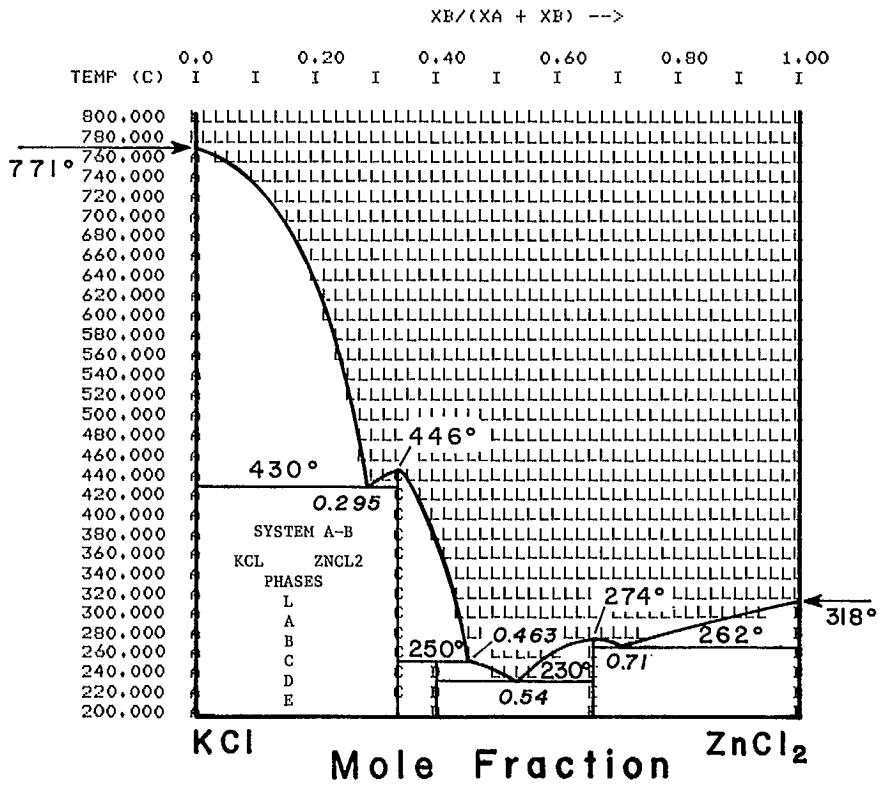

TEMP (C)	Compositions, in mole fractions, of phase boundaries								
800.000									
780.000									
760.000	0.0	0.04736							
740.000	0.0	0.10889							
720.000	0.0	0.13818							
700.000	0.0	0.15967							
680.000	0.0	0.17725							
660.000	0.0	0.19189							
640.000	0.0	0.20557							
620.000	0.0	0.21729							
600.000	0.0	0.22803							
580.000	0.0	0.23877							
560.000	0.0	0.24756							
540.000	0.0	0.25635							
520.000	0.0	0.26416							
500.000	0.0	0.27197							
480.000	0.0	0.27979							
460.000	0.0	0.28662							
440.000	0.0	0.29295	0.31054	0.33333	0.33333	0.35612			
420.000	0.0	0.33333	0.33333	0.38086					
400.000	0.0	0.33333	0.33333	0.39648					
380.000	0.0	0.33333	0.33333	0.40950					
360.000	0.0	0.33333	0.33333	0.42122					
340.000	0.0	0.33333	0.33333	0.43034					
320.000	0.0	0.33333	0.33333	0.43945					
300.000	0.0	0.33333	0.33333	0.44736	0.93213	1.00000			
280.000	0.0	0.33333	0.33333	0.45507	0.74072	1.00000			
260.000	0.0	0.33333	0.33333	0.46116	0.59831	0.66667	0.66667	1.00000	
240.000	0.0	0.33333	0.33333	0.40000	0.40000	0.50586	0.55664	0.66667	0.66667	1.00000
220.000	0.0	0.33333	0.33333	0.40000	0.40000	0.66667	0.66667	1.00000		
200.000	0.0	0.40000	0.40000	0.66667	0.66667	1.00000				

KCl-ZnCl₂

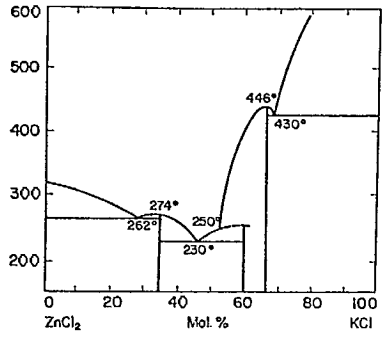

FIG. 1273.—System KCl–$ZnCl_2$.
Yu A. Ugai and V. A. Shatillo, *J. Phys. Chem. U.S.S.R.*, 23 [6] 745 (1949). See also F. R. Duke and R. A. Fleming, *J. Electrochem. Soc.*, 104, 253 (1957.)

Fig. A-4 - Calculated and measured phase diagrams for $KCl-ZnCl_2$

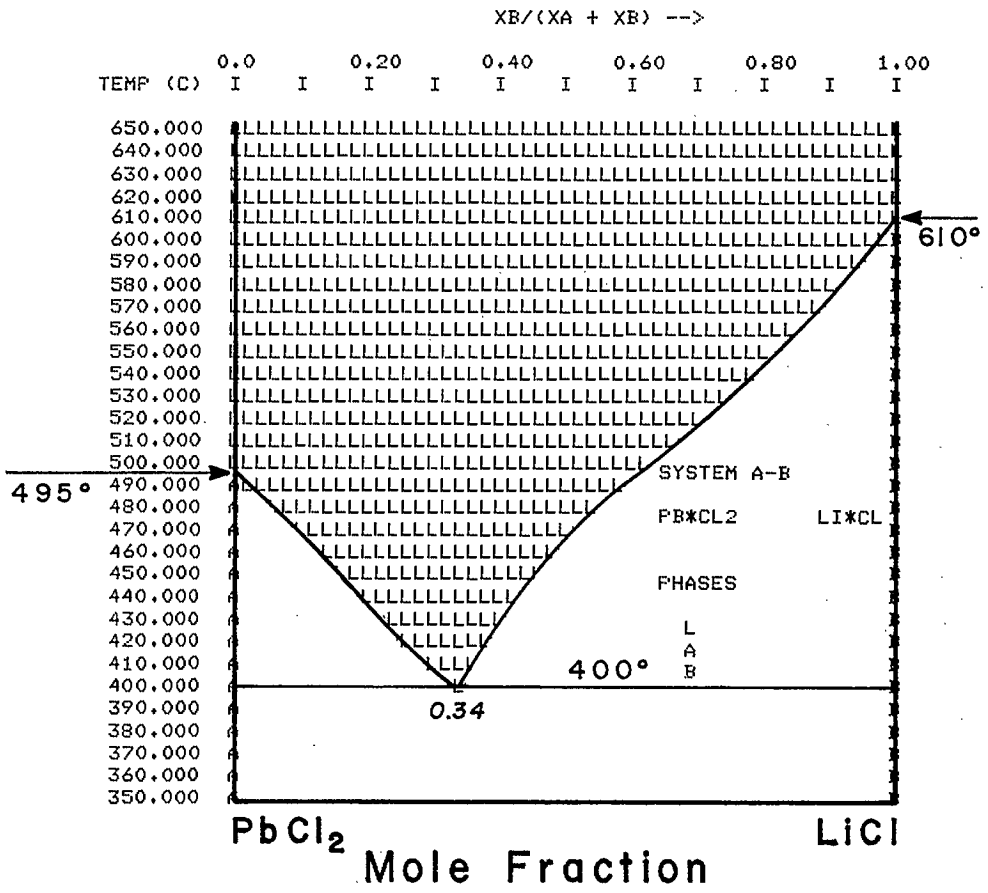

Fig. A-5 - Calculated and measured phase diagrams for $LiCl-PbCl_2$

TEMP (C)	Compositions, in mole fractions, of phase boundaries			
650.000				
640.000				
630.000				
620.000				
610.000				
600.000	0.97021	1.00000		
590.000	0.93896	1.00000		
580.000	0.90771	1.00000		
570.000	0.87549	1.00000		
560.000	0.84229	1.00000		
550.000	0.80811	1.00000		
540.000	0.77100	1.00000		
530.000	0.73291	1.00000		
520.000	0.69385	1.00000		
510.000	0.65381	1.00000		
500.000	0.61475	1.00000		
490.000	0.0	0.02422	0.57666	1.00000
480.000	0.0	0.06399	0.54150	1.00000
470.000	0.0	0.09977	0.50830	1.00000
460.000	0.0	0.13304	0.47803	1.00000
450.000	0.0	0.16637	0.45068	1.00000
440.000	0.0	0.20019	0.42529	1.00000
430.000	0.0	0.23254	0.40088	1.00000
420.000	0.0	0.26750	0.37939	1.00000
410.000	0.0	0.30293	0.35986	1.00000
400.000	0.0	0.33967	0.34033	1.00000
390.000	0.0	1.00000		
380.000	0.0	1.00000		
370.000	0.0	1.00000		
360.000	0.0	1.00000		
350.000	0.0	1.00000		

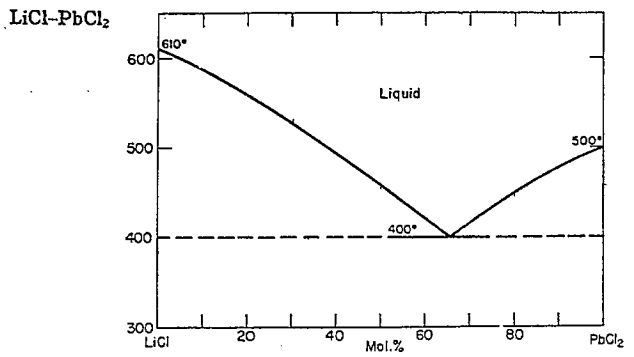

FIG. 3089.—System $LiCl-PbCl_2$.

S. P. Gromakov and L. M. Gromakova, *Zh. Fiz. Khim.*, 29 [4] 747 (1955). See also G. A. Bukhalova and N. N. Aleshkina, *Dokl. Akad. Nauk SSSR*, 88, 819 (1953).

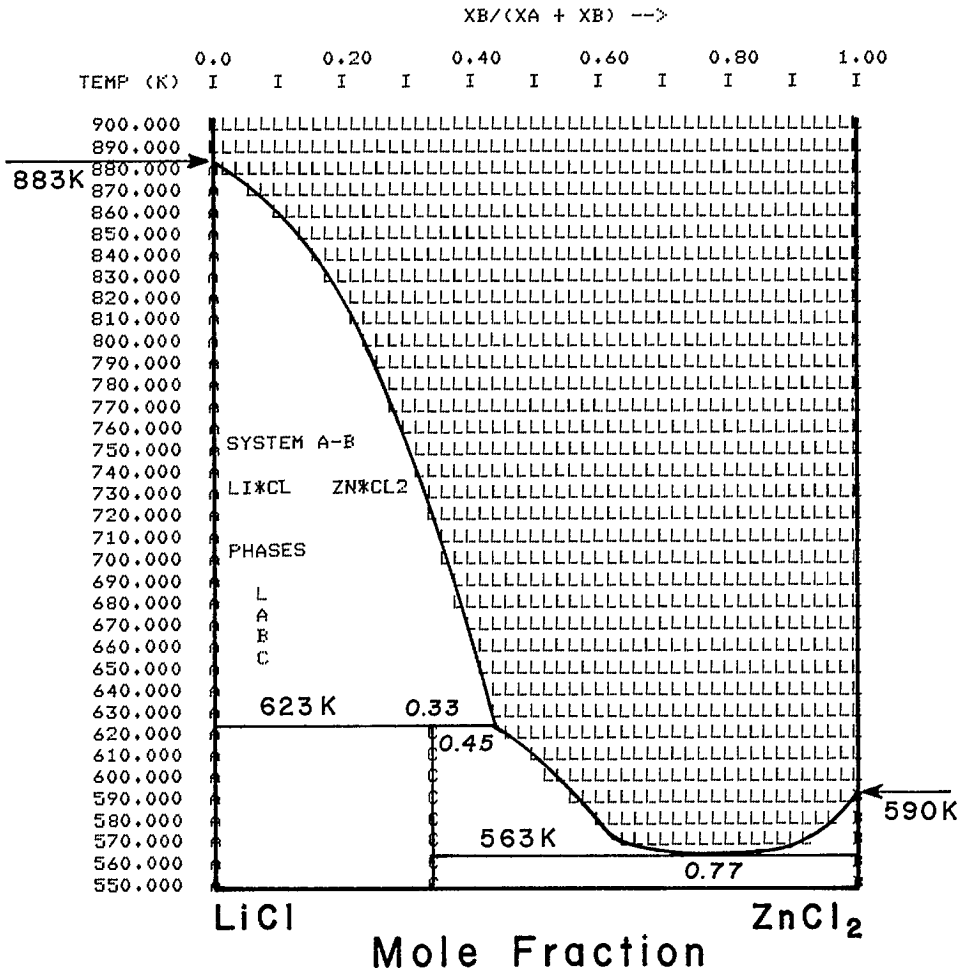

TEMP (K)	Compositions, in mole fractions, of phase boundaries					
900.000						
890.000						
880.000	0.0	0.01025				
870.000	0.0	0.05127				
860.000	0.0	0.09912				
850.000	0.0	0.13721				
840.000	0.0	0.16650				
830.000	0.0	0.18994				
820.000	0.0	0.21045				
810.000	0.0	0.22803				
800.000	0.0	0.24463				
790.000	0.0	0.25928				
780.000	0.0	0.27295				
770.000	0.0	0.28662				
760.000	0.0	0.29932				
750.000	0.0	0.31201				
740.000	0.0	0.32373				
730.000	0.0	0.33447				
720.000	0.0	0.34619				
710.000	0.0	0.35693				
700.000	0.0	0.36768				
690.000	0.0	0.37842				
680.000	0.0	0.38916				
670.000	0.0	0.39990				
660.000	0.0	0.41064				
650.000	0.0	0.42041				
640.000	0.0	0.43115				
630.000	0.0	0.44189				
620.000	0.0	0.33333	0.33333	0.46159		
610.000	0.0	0.33333	0.33333	0.49544		
600.000	0.0	0.33333	0.33333	0.52669		
590.000	0.0	0.33333	0.33333	0.56067	0.99658	1.00000
580.000	0.0	0.33333	0.33333	0.59687	0.95947	1.00000
570.000	0.0	0.33333	0.33333	0.64736	0.91064	1.00000
560.000	0.0	0.33333	0.33333	1.00000		
550.000	0.0	0.33333	0.33333	1.00000		

Fig. A-6 - Calculated and measured phase diagrams for $LiCl-ZnCl_2$

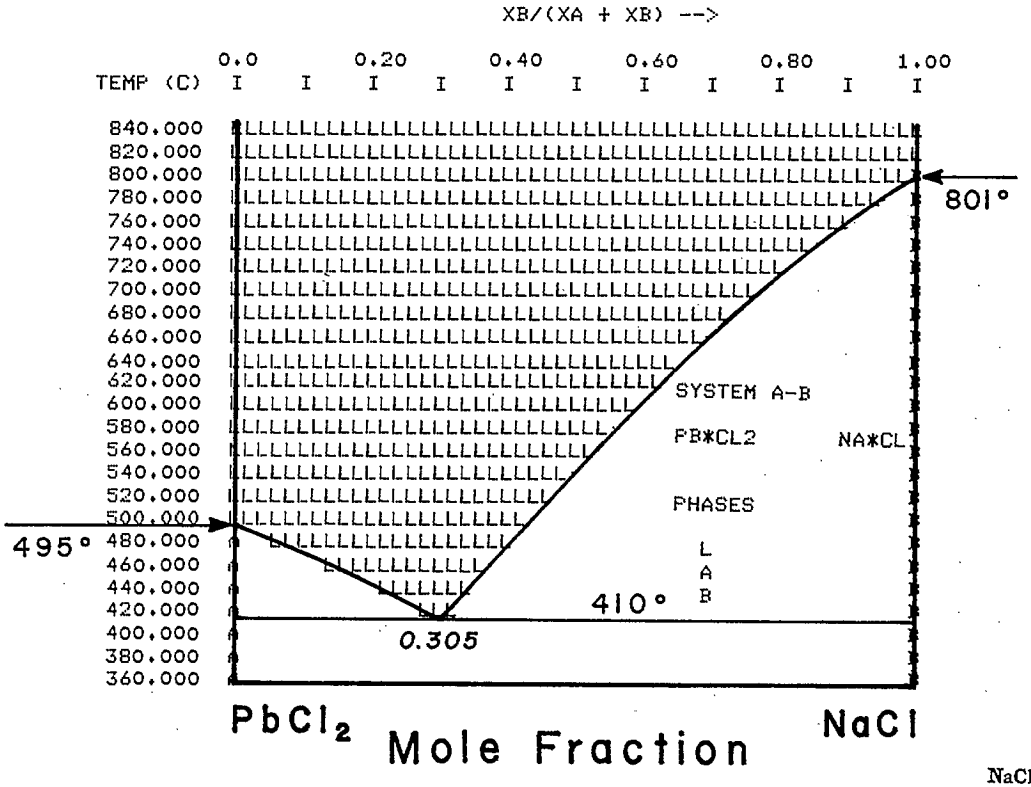

TEMP (C)	Compositions, in mole fractions, of phase boundaries			
840.000				
820.000				
800.000	0.99854	1.00000		
780.000	0.94287	1.00000		
760.000	0.89307	1.00000		
740.000	0.84619	1.00000		
720.000	0.80322	1.00000		
700.000	0.76221	1.00000		
680.000	0.72314	1.00000		
660.000	0.68506	1.00000		
640.000	0.64893	1.00000		
620.000	0.61475	1.00000		
600.000	0.58057	1.00000		
580.000	0.54834	1.00000		
560.000	0.51611	1.00000		
540.000	0.48486	1.00000		
520.000	0.45557	1.00000		
500.000	0.42627	1.00000		
480.000	0.0	0.06917	0.39795	1.00000
460.000	0.0	0.14511	0.36963	1.00000
440.000	0.0	0.21326	0.34229	1.00000
420.000	0.0	0.27543	0.31689	1.00000
400.000	0.0	1.00000		
380.000	0.0	1.00000		
360.000	0.0	1.00000		

Fig. A-7 - Calculated and measured phase diagrams for $NaCl-PbCl_2$

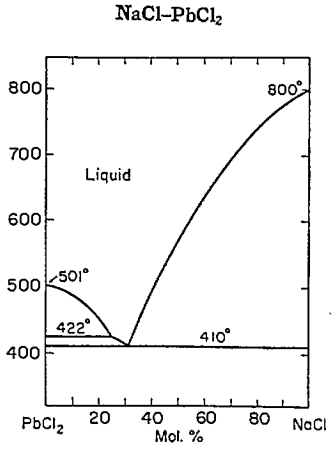

FIG. 3104.—System NaCl–PbCl .

T. N. Sumarokova and T. P. Modestova, *Zh. Neorgan. Khim.*, 6 [3] 679 (1961); *Russ. J. Inorg. Chem.* (*English Transl.*), 346 (1961).

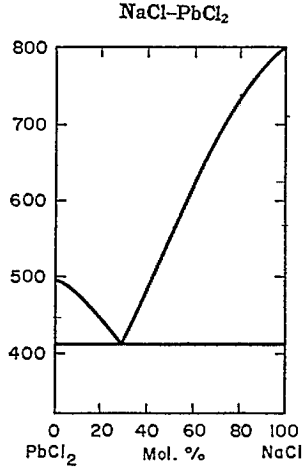

FIG. 1310.—System $NaCl–PbCl_2$.

Kurt Treis, *Neues Jahrb. Mineral., Geol.*, **37**, 772 (1914)

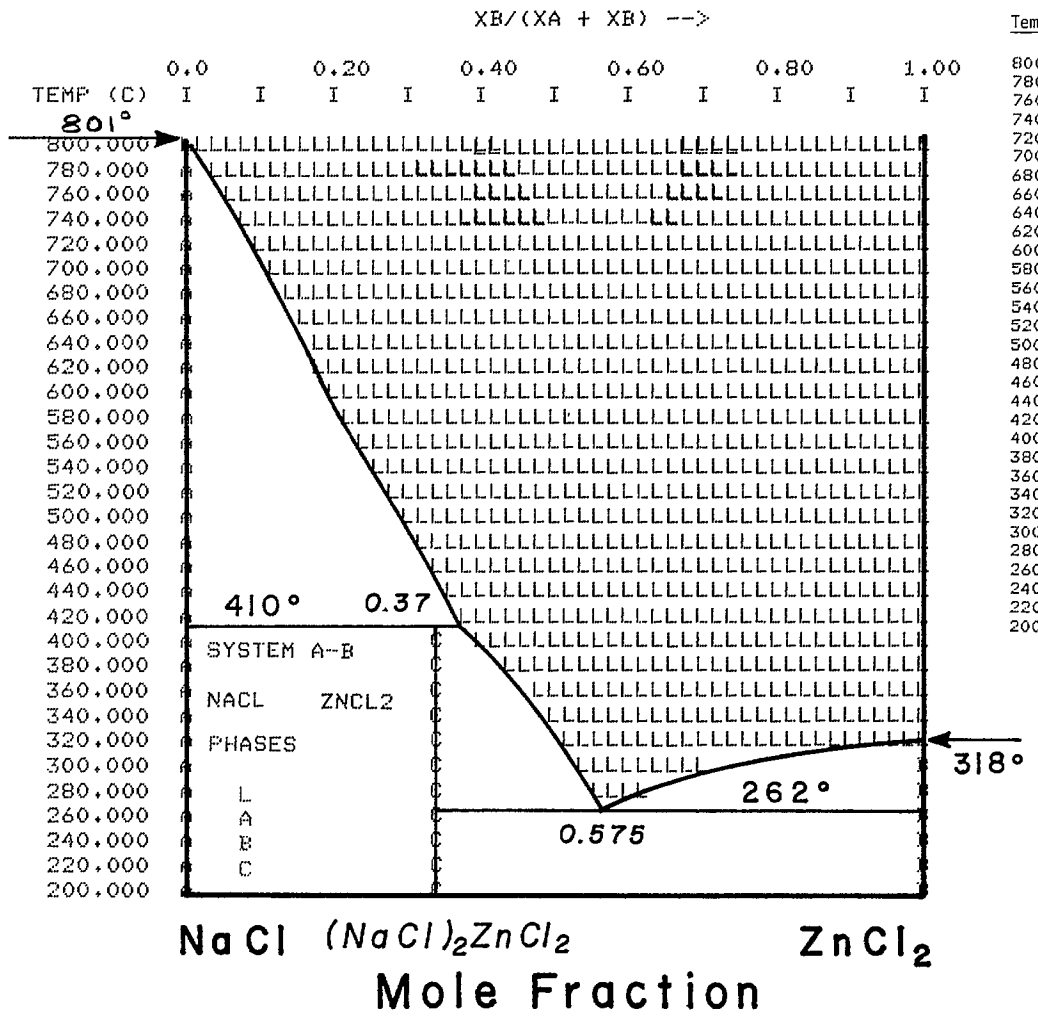

Fig. A-8 - Calculated and measured phase diagrams for $NaCl-ZnCl_2$

Temp (C)	Compositions, in mole fractions, of phase boundaries					
800.000	0.0	0.00146				
780.000	0.0	0.03662				
760.000	0.0	0.06006				
740.000	0.0	0.08057				
720.000	0.0	0.10010				
700.000	0.0	0.11768				
680.000	0.0	0.13525				
660.000	0.0	0.15283				
640.000	0.0	0.17041				
620.000	0.0	0.18799				
600.000	0.0	0.20557				
580.000	0.0	0.22314				
560.000	0.0	0.24170				
540.000	0.0	0.26025				
520.000	0.0	0.27881				
500.000	0.0	0.29736				
480.000	0.0	0.31592				
460.000	0.0	0.33447				
440.000	0.0	0.35303				
420.000	0.0	0.37061				
400.000	0.0	0.33333	0.33333	0.40299		
380.000	0.0	0.33333	0.33333	0.44205		
360.000	0.0	0.33333	0.33333	0.47200		
340.000	0.0	0.33333	0.33333	0.49804		
320.000	0.0	0.33333	0.33333	0.52148		
300.000	0.0	0.33333	0.33333	0.54244	0.69873	1.00000
280.000	0.0	0.33333	0.33333	0.56143	0.61475	1.00000
260.000	0.0	0.33333	0.33333	1.00000		
240.000	0.0	0.33333	0.33333	1.00000		
220.000	0.0	0.33333	0.33333	1.00000		
200.000	0.0	0.33333	0.33333	1.00000		

$NaCl-ZnCl_2$

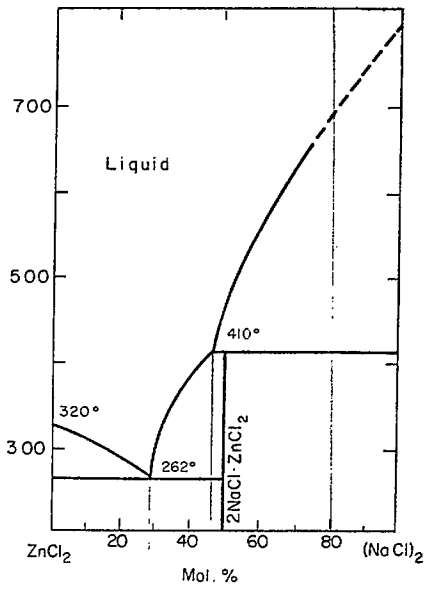

FIG. 3106.—System $(NaCl)_2$–$ZnCl_2$.

N. N. Evseeva and A. G. Bergman, *Izv. Sektora Fiz.-Khim. Analiza, Inst. Obshch. Neorgan. Khim., Akad. Nauk SSSR*, 21, 212 (1952).

APPENDIX B - ISOTHERMAL SECTIONS OF TERNARY PHASE DIAGRAMS*

*The phases in the isothermal sections of this appendix may be identified by referring to the appropriate polythermal projections of Fig. 2-5. The edges of the composition triangles in this appendix are graduated in mole percentages.

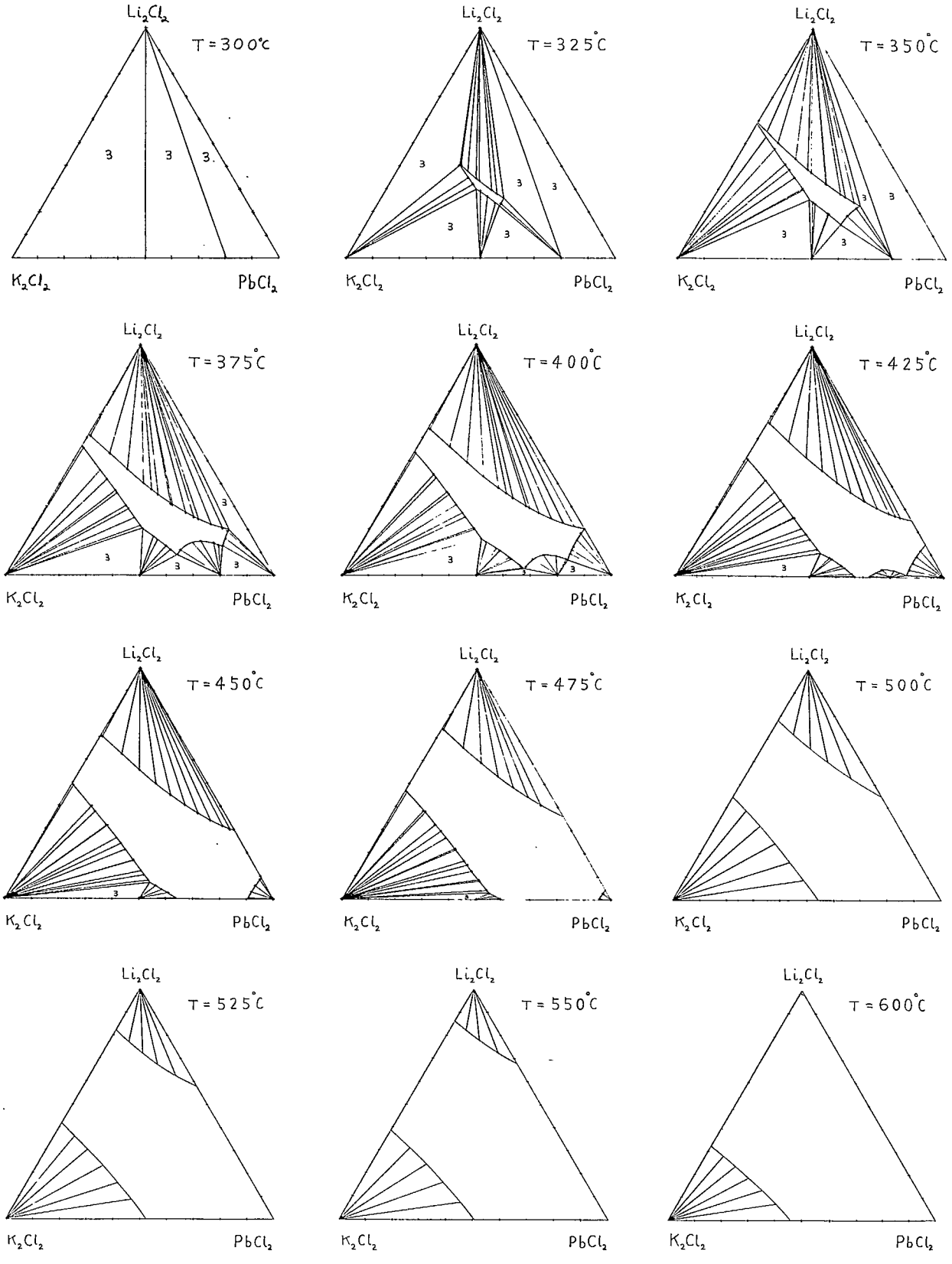

Fig. B-1 - Isothermal sections of ternary phase diagrams for $LiCl-KCl-PbCl_2$ (300°C, 325°C, 350°C .... 600°C)

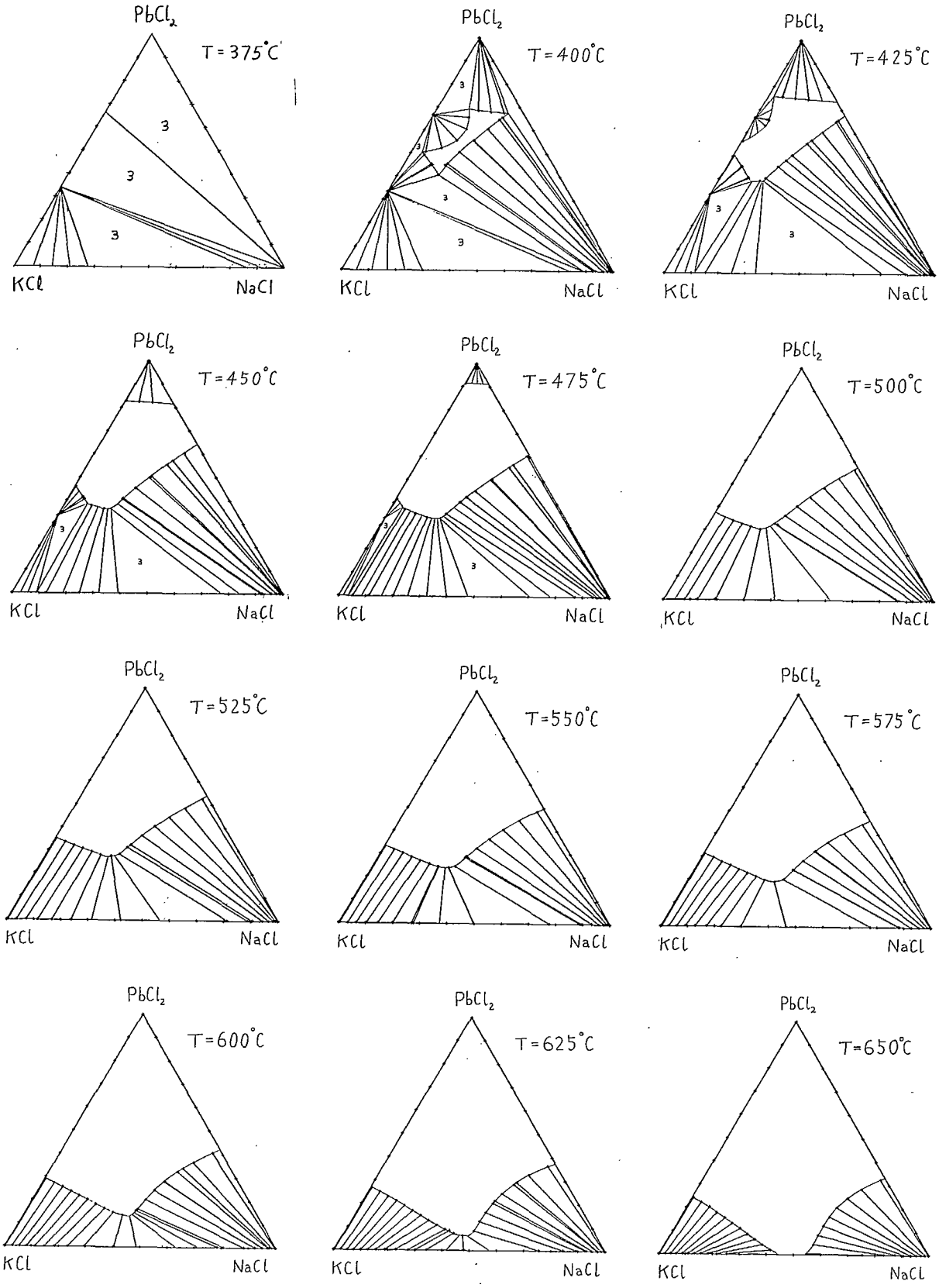

Fig. B-2 - Isothermal sections of ternary phase diagrams for $NaCl-KCl-PbCl_2$ (375°C, 400°C, 425°C, ... 650°C)

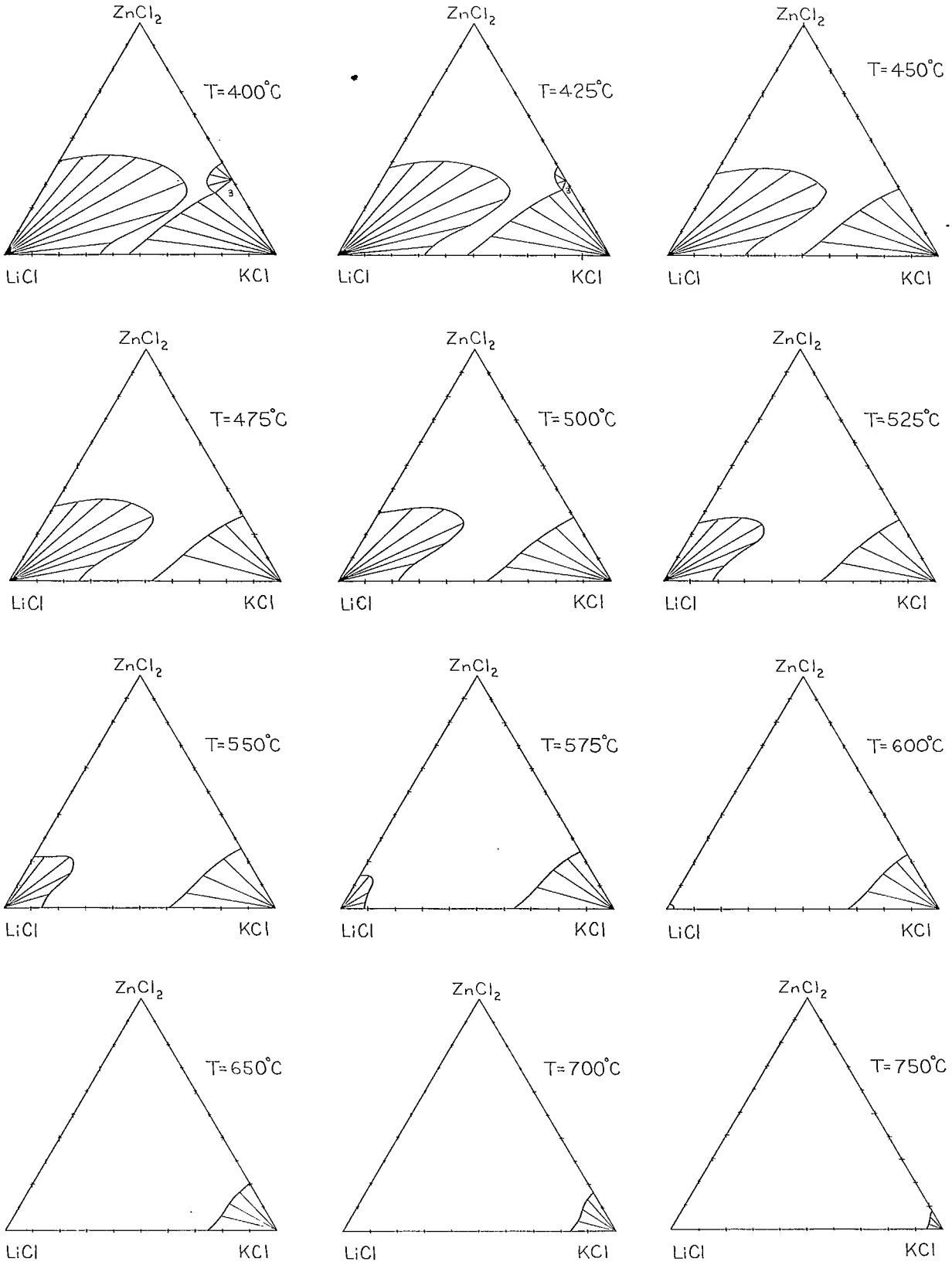

Fig. B-3 - Isothermal sections of ternary phase diagrams for $LiCl-KCl-ZnCl_2$ (400°C, 425°C, ... 600°C, 650°C, 700°C, 750°C)

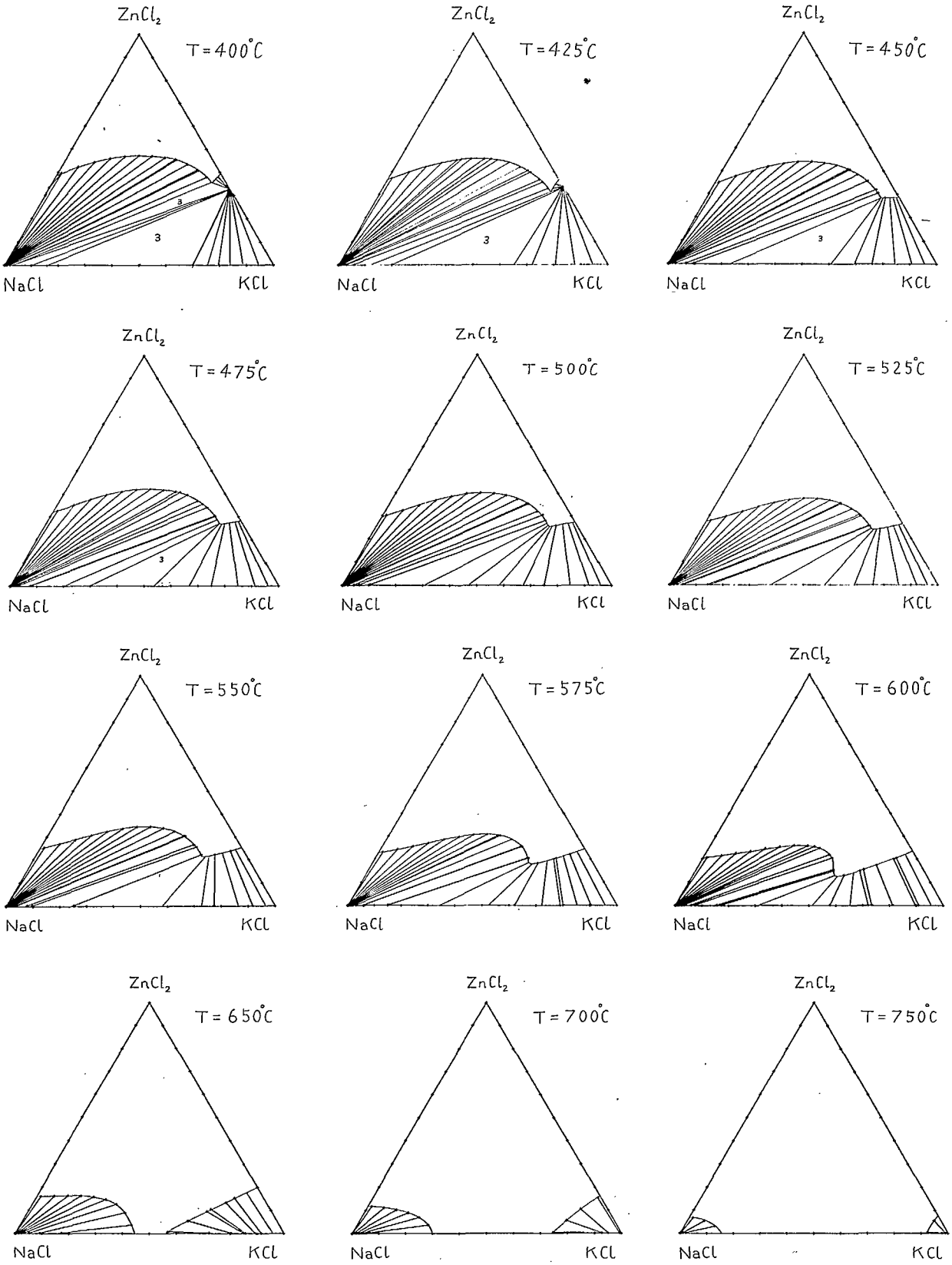

Fig. B-4 - Isothermal sections of ternary phase diagrams for $NaCl-KCl-ZnCl_2$ (400°C, 425°C, ... 600°C, 650°C, 700°C, 750°C)

APPENDIX C - TERNARY ISO-ACTIVITY CURVES*

*Some of the low temperature iso-activity lines represent activities of the base metal chloride in a metastable liquid at temperatures below the liquidus surface. The edges of the composition triangles in this appendix are graduated in mole percentages.

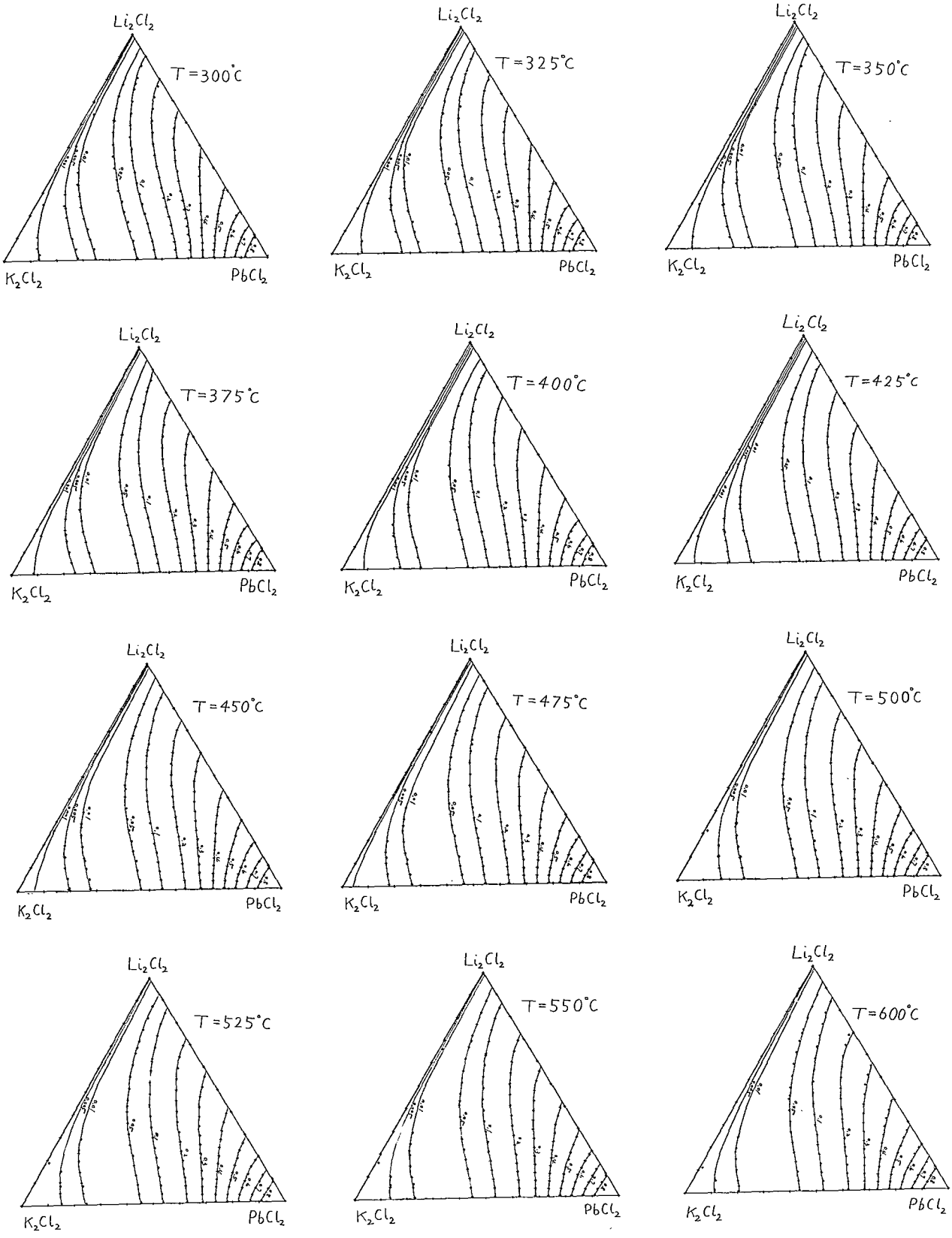

Fig. C-1 - Ternary iso-activity curves for $LiCl-KCl-PbCl_2$ a_{PbCl_2} (300°C, 325°C ... 600°C)

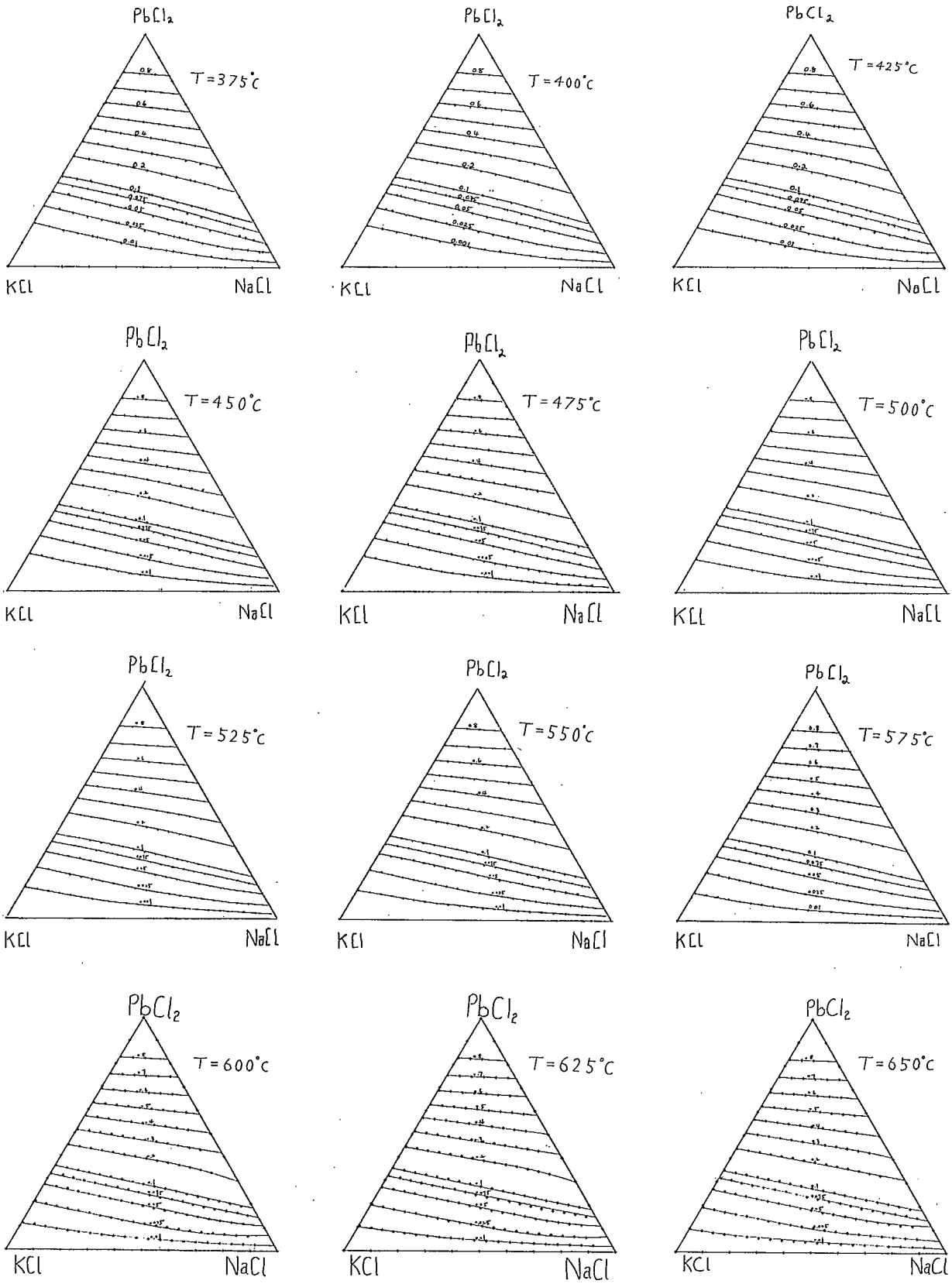

Fig. C-2 - Ternary iso-activity curves for NaCl-KCl-$PbCl_2$
a_{PbCl_2} (375°C, 400°C ... 650°C)

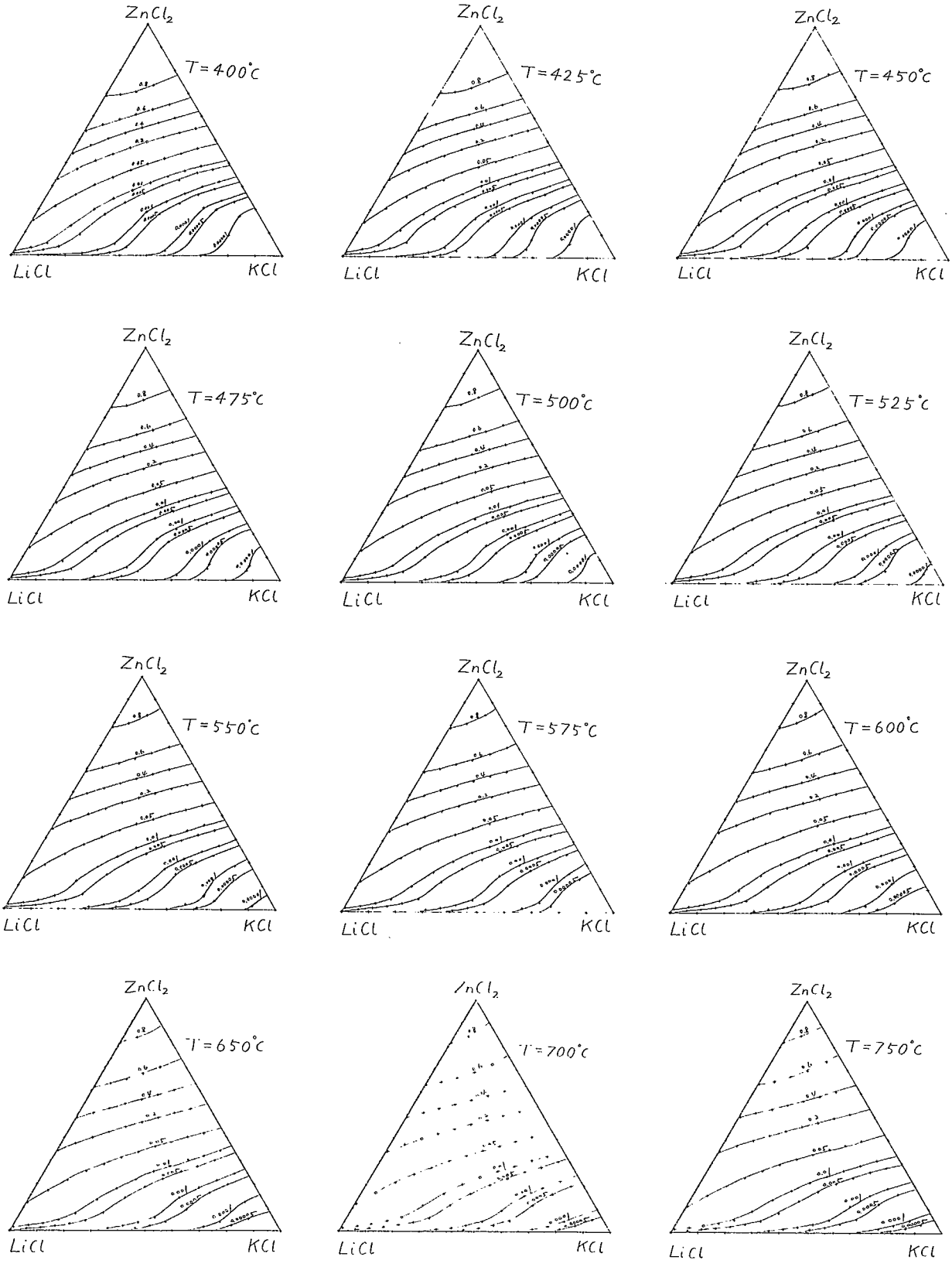

Fig. C-3 - Ternary iso-activity curves for LiCl-KCl-$ZnCl_2$
a_{ZnCl_2} (400°C, 425°C ... 600°C, 650°C, 700°C, 750°C)

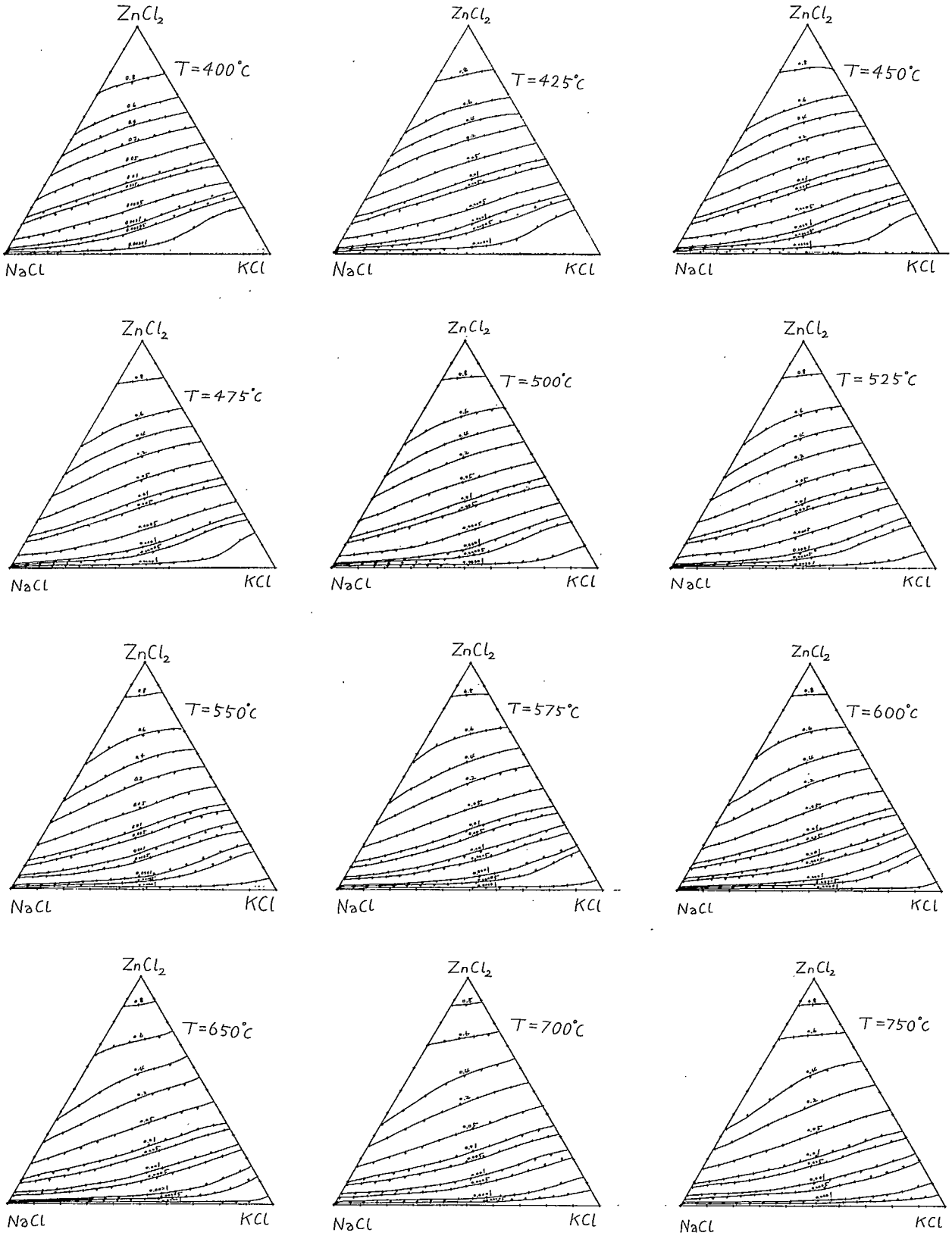

Fig. C-4 - Ternary iso-activity curves for NaCl-KCl-$ZnCl_2$
a_{ZnCl_2} (400°C, 425°C ... 600°C, 650°C, 700°C, 750°C)

CANMET REPORTS

Recent CANMET reports presently available or soon to be released through Printing and Publishing, Supply and Services, Canada (addresses on inside front cover), or from CANMET Publications Office, 555 Booth Street, Ottawa, Ontario, K1A 0G1:

Les récents rapports de CANMET, qui sont présentement disponibles ou qui le seront bientôt peuvent être obtenus de la direction de l'Imprimerie et de l'Edition, Approvisionnements et Services Canada (adresses au verso de la page couverture), ou du Bureau de vente et distribution de CANMET, 555, rue Booth, Ottawa, Ontario, K1A 0G1:

79-8 Flotation techniques for producing high-recovery bulk Zn-Pb-Cu-Ag concentrate from a New Brunswick massive sulphide ore; A.I. Stemerowicz and G.W. Leigh;
Cat. No. M38-13/79-8, ISBN 0-660-10448-2; Price: $8.00 Canada, $9.60 other countries.

79-10 A comparative study of lightweight aggregates in structural concrete; H.S. Wilson;
Cat. No. M38-13/79-10, ISBN 0-660-10449-0; Price: $2.00 Canada, $2.40 other countries.

79-11 CANMET's rock mechanics research at the Kid Creek mine; D.G.F. Hedley, G. Herget, P. Miles and Y.S. Yu;
Cat. No. M38-13/79-11, ISBN 0-660-10472-5; Price: $3.50 Canada, $4.20 other countries.

79-17 Rapid chromatographic procedure for characterizing hydrocarbons in synthetic fuel naphtha; A.E. George, G.T. Smiley and H. Sawatzky;
Cat. No. M38-13/79-17, ISBN 0-660-10428-8; Price: $2.75 Canada, $3.30 other countries.

79-18 Influence of flue temperature and coal preparation on coke quality in 460-mm technical scale coke oven; J.F. Gransden and W.R. Leeder;
Cat. No. M38-13/79-18, ISBN 0-660-10441-5; Price: $1.50 Canada, $1.80 other countries.

79-20 Effect of hydrocracking on the distribution of nitrogenous components in Athabasca bitumen; H. Sawatzky, J.E. Beshai, G.T. Smiley and A.E. George;
Cat. No. M38-13/79-20, ISBN 0-660-10442-3; Price: $1.25 Canada, $1.50 other countries.

79-25 CANMET review 1978-79; Staff of CANMET;
Cat. No. M38-13/79-25, ISBN 0-660-10522-5; Price: $4.25 Canada, $5.10 other countries.

79-28 Sulphur concrete and sulphur infiltrated concrete: Properties, applications and limitations; V.M. Malhotra;
Cat. No. M38-13/79-28, ISBN 0-660-10469-5; Price: $2.25 Canada, $2.70 other countries.

79-29 Geological disposal of high-level radioactive wastes; D.F. Coates, G. Larocque and L. Geller; (Policy paper);
Cat. No. M38-13/79-29, ISBN 0-660-10523-3; Price: $1.50 Canada, $1.80 other countries.

79-30 In situ testing for concrete strength; V.M. Malhotra and G.G. Carette;
Cat. No. M38-13/79-30, ISBN 0-660-10506-3; Price: $1.75 Canada, $2.10 other countries.

79-31 Superplasticizers: Their effect on fresh and hardened concrete; V.M. Malhotra;
Cat. No. M38-13/79-31, ISBN 0-660-10530-6; Price: $2.00 Canada, $2.40 other countries.

79-32 Concrete made with supplementary cementing materials; E.E. Berry;
Cat. No. M38-13/79-32, ISBN 0-660-10470-9; Price: $2.25 Canada, $2.70 other countries.

79-33 Lightweight aggregates: Properties, applications and outlook; H.S. Wilson;
Cat. No. M38-13/79-33, ISBN 0-660-10482-2; Price: $2.25 Canada, $2.70 other countries.